Journal of Environmental Management 350 (2024) 119567

Contents lists available at ScienceDirect

Journal of Environmental Management

journal homepage: www.elsevier.com/locate/jenvman

Research article

Hazardous waste management (Buxus papillosa) investment for the prosperity of environment and circular economy: Response surface methodology-based simulation

Ikram Faiz [a], Mushtaq Ahmad [a,***], Mohamed Fawzy Ramadan [b], Ulfat Zia [a], Rozina [a], Awais Bokhari [c,d,e], Saira Asif [f,**], Andrea Pieroni [g,h], Sasan Zahmatkesh [i,j,*], Bing-Jie Ni [k]

[a] Department of Plant Sciences, Quaid-i-Azam University Islamabad, 45320, Pakistan
[b] Department of Clinical Nutrition, Faculty of Applied Medical Sciences, Umm Al-Qura University, Makkah, Kingdom of Saudi Arabia
[c] Department of Chemical Engineering, COMSATS University Islamabad (CUI), Lahore Campus, 54000, Lahore, Punjab, Pakistan
[d] School of Engineering, Lebanese American University, Byblos, Lebanon
[e] Sustainable Process Integration Laboratory, SPIL, NETME Centra, Faculty of Mechanical Engineering, Brno University of Technology, VUT Brno, Technická 2896/2, Brno, 616 00, Czech Republic
[f] Faculty of Sciences, Department of Botany, PMAS Arid Agriculture University, Rawalpindi, Pakistan
[g] University of Gastronomic Sciences, Piazza Vittorio Emanuele II 9, 12042, Pollenzo, Italy
[h] Department of Medical Analysis, Tishk International University, Erbil 44001, Kurdistan, Iraq
[i] Tecnologico de Monterrey, Escuela de Ingenieríay Ciencias, Puebla, Mexico
[j] Faculty of Health and Life Sciences, INTI International University, 71800, Nilai, Negeri Sembilan, Malaysia
[k] School of Civil and Environmental Engineering, The University of New South Wales, Sydney, NSW, 2052, Australia

ARTICLE INFO

Handling Editor: Raf Dewil

Keywords:
Hazardous waste management
Buxus papillosa
Response surface methodology
Fuel
Phyto-nanocatalyst
Biodiesel

ABSTRACT

Dealing with the current defaults of environmental toxicity, heating, waste management, and economic crises, exploration of novel non-edible, toxic, and waste feedstock for renewable biodiesel synthesis is the need of the hour. The present study is concerned with Buxus papillosa with seeds oil concentration (45% w/w), a promising biodiesel feedstock encountering environmental defaults and waste management; in addition, this research performed simulation based-response surface methodology (RSM) for *Buxus papillosa* bio-diesel. Synthesis and application of novel Phyto-nanocatalyst bimetallic oxide with Buxus papillosa fruit capsule aqueous extract was advantageous during transesterification. Characterization of sodium/potassium oxide Phyto-nanocatalyst confirmed 23.5 nm nano-size and enhanced catalytic activity. Other characterizing tools are FTIR, DRS, XRD, Zeta potential, SEM, and EDX. Methyl ester formation was authenticated by FTIR, GC-MS, and NMR. A maximum 97% yield was obtained at optimized conditions i.e., methanol ratio to oil (8:1), catalyst amount (0.37 wt%), reaction duration (180 min), and temperature of 80 °C. The reusability of novel sodium/potassium oxide was checked for six reactions. *Buxus papillosa* fuel properties were within the international restrictions of fuel. The sulphur content of 0.00090% signified the environmental remedial nature of *Buxus papillosa* methyl esters and it is a highly recommendable species for biodiesel production at large scale due to a t huge number of seeds production and vast distribution.

1. Introduction

Swift global outgrowth along with the expeditious growth rate of the human population has increased energy, water, and food insecurities (Mahlknecht et al., 2020). The Pandemic COVID-19 and rapid climatic change brought more scarcity of these natural resources in certain regions of the world (Udmale et al., 2020). The drastic weather changes globally have increased the vulnerability to floods. Durner mentioned in 2009 that South Asia is likely to suffer from floods as climate change is adversely affecting tropical cyclones and Monsoon patterns (Durner et al., 2009). The recent flood of 2022 in Pakistan has affected 33 million

* Corresponding author. Tecnologico de Monterrey, Escuela de Ingenieríay Ciencias, Puebla, Mexico.
** Corresponding author.
*** Corresponding author.
E-mail addresses: mushtaq@qau.edu.pk (M. Ahmad), sairaasif@uaar.edu.pk (S. Asif), sasan_zahmatkesh@yahoo.com (S. Zahmatkesh).

https://doi.org/10.1016/j.jenvman.2023.119567
Received 27 July 2023; Received in revised form 25 October 2023; Accepted 4 November 2023
Available online 25 November 2023

Abbreviations

BP	*Buxus papillosa*
BPBD	*Buxus papillosa* biodiesel
CCD	Central composite design
BPO	*Buxus papillosa* oil
FFA	Free fatty acids
FAME	Fatty acid methyl esters
Na/KO	Sodium Potassium oxide
NPs	Nanoparticles
XRD	X-ray diffraction
SEM	Scanning electron microscopy
EDS	Energy dispersive spectroscopy
DRS	Diffuse reflectance spectroscopy
FTIR	Fourier transforms infrared spectroscopy
RSM	Response surface methodology
ANOVA	Analysis of variance
GS-MS	Gas and mass spectroscopy
NMR	Nuclear magnetic resonance
ZP:	Zeta potential

people and destroyed millions of hectares of food crops cultivated in fields that directly lead to food and fuel crises and price increments (He et al., 2023). A loss of 30 billion dollars has damaged Pakistan's economy (Devi, 2022). Due to a tremendous increase in the inflation rate, the prices of fossil fuels have doubled during the past two to three years. The ultimate reason for the price hack is a change in climate leading to floods and other natural disasters, non-renewability, and pollution of fossil fuels. Green fuel with its more friendly qualities towards the environment, renewability, low cost and sustaining can combat the fuel-related energy crises and climate change (Ahmad et al., 2022a). In these prevailing crises, the concept of circular economy must be installed in every field to ensure a sustainable environment and deal with such pathetic situations.

Oils from edible vegetable feedstock is used for biodiesel production that competes with food issues (Kurowska et al., 2020). As food is a basic and foremost necessity of life for humans and other living beings, the trend from edible seed oil changed towards non-edible, wild plant seed oil (Ewing and Msangi, 2009). According to FAO report 2022, from all over the world around two billion people are suffering from hunger (Arora and Mishra, 2022). Wild, non-edible plant seeds oil also decreases the cost of biofuel production as 80% of the cost is high due to the high prices of edible feedstock. For biodiesel production, non-edible and wild plant seeds oil is a reliable alternate source as less water, nutrients and proper land management is not required (Fadhil et al., 2020). Such plant can be grown along roadside, along the crop's fields and unwanted barren lands (Yesilyurt and Cesur, 2020). Production of biodiesel for the transport sector is a turning point for energy crises as in one calendar year the total consumption of fossil fuel is 500 EJ all over the world. In the future, it will be significantly used in technical and academic studies because of its outstanding nonlinear simulation capability (Ahmad, 2022), fault-tolerant nature, and capacity for independent learning (Aikhuele. 2023). The optimum biodiesel produced in a spiral-shaped processor at super-critical temperatures was identified using an artificial neural networks (ANN) technique (Deng et al., 2022; Hu et al., 2022; Meng et al., 2022). An ANN system (Wang et al., 2023) was implemented to forecast the distribution of Ricinus communis seed biodiesel testing results.

More inquisition for non-edible seeds is required in order to investigate more plants for seed oil content. *Buxus papillosa* has a good potential for biodiesel production as its seeds has 45% oil content. It belongs to Family Buxaceae. The plant body is often a shrub or short heighted tree. Straightened branching system grows along a crooked stem. Leaves length is 1.5–5.5 cm and width vary from 0.5 to 1.2 cm. Leaf shape is either oblongly elliptical or narrow-lanceolate having a minor leaf stalk. Veins are not prominent (Saleem et al., 2022). Capsules are walnut-brown colored, trilocular and oval to oblong-shaped with upright horns. The seeds are black, oblong-shaped, with a length of 4 mm and width 3 mm (Gupta, 2010).

Biofuels are produced by various methodologies and techniques that include co-pyrolysis, pyrolysis, transesterification, dilution and micro-emulsification etc. (Marchetti et al., 2007). Catalytic activity is crucial to biodiesel production as it minimize the time duration by speed up reaction, lowering the activation energy for the reaction (Sanjay, 2013). Catalysts can be recycled as they do not consumed during the reaction (Wang et al., 2017). Without catalytic activity, transesterification is a time-consuming process. Different catalysts such heterogenous, homogenous and enzyme based catalytic activity are employed for transesterification process to bring about biodiesel production. Homogenous catalysts are associated with some environment non-friendly by products such as giant chemical waste, low yield percentage and non-recyclable that further affect environment and fuel prices (Jayakumar et al., 2021). They have corrosive nature, can damage the reaction machinery. Heterogenous are oxides of metals and associated complexes. They perform more vigorously when conditions are optimal (Di Serio et al., 2008). Enzymatic and heterogenous catalysts show resistance in mass transfer and reusability.

Green nano catalyst is combating all the challenges associated with the other types of catalysts in biofuel preparation. Green nano-catalyst shows more catalytic activity, stability and reliable reusability as they have high surface area (Zhang et al., 2020). Various parts of plants are utilized for green nano catalyst synthesis because of presence of naturally occurring reducing agents, stabilizing agents, different enzymes and metabolites that also serves in reducing stabilizing activities (Ahmad et al., 2022b).

Transesterification is carried through various reactors such as cavitation reactor, microwave reactor, spinning tube reactor, oscillatory flow reactor and membrane reactor (Bhatia et al., 2021). Out of these reactors only membrane reactor is proficient to overwhelm the chemical equilibrium limitations during transesterification. Membrane-based reactive separator incorporates the reaction and separation in a single chamber and results in the high yield and specificity of the reaction (Gómez-Trejo-López et al., 2022). Membrane reactor avoids intermediate steps and thus biodiesel production is made more cost effective. Membrane based reactor being a trustworthy, economical technology of biodiesel production is applied mostly to carry out transesterification process (Kumar et al., 2020).

In order to avoid dangerous chemicals and their effects on environment caused by nanoparticles synthesis via chemical methods, the capital concern of the present research work is the synthesis of novel Na/K–O by utilizing Sodium–Potassium tartrate salt along with the green extract of *Buxus papillosa* fruit covering. In the previous literature there is no evidence of Sodium Potassium tartrate nanoparticles and *Buxus papillosa* fruit covering extract. Fruit covering is usually a waste part of this plant as falls off on ripening. The central aim connected with this research is greener, uneatable, wild, non-pollutant, waste management, non-toxic and low-cost biodiesel production from *Buxus papillosa* seeds being noncompeting with food resources, minimize the emission of pollutant gases thus repairing the climate change.

A chain of experiments was performed for converting nonedible seed oil of *Buxus papillosa* into fatty acid methyl esters (FAMEs) utilizing newly formed nano catalyst and their effectiveness was checked through Response surface methodology (RSM). The green nano catalyst was characterized through several analytical techniques such FTIR, SEM, EDX, XRD, Zeta potential and DRS. Innovatory characterization techniques such as GC/MS, FTIR and NMR (^{1}H and ^{13}C) were applied for methyl esters characterization.

2. Research methodology

2.1. Plant collection

Seeds of *Buxus papillosa* were collected during multiple field visits in the months of July and August from the Margalla hills zone of the lesser Himalayas, Islamabad (Pakistan). The plant sample was recognized by well-knowledgeable taxonomists and compared with herbarium-dried specimens preserved in the herbarium of Pakistan (ISL) for further affirmation. The process of seed drying was done under shade at a room temperature of 35 °C to lessen the moisture level for one week (Abbasi et al., 2023).

2.2. Oil content determination

To ensure complete water content removal, seeds were placed inside the oven at 60 °C for one day to attain the exact seed oil content (Arshad et al., 2023). Seeds were crushed into finely powdered condition with the help of a mortar and pestle. Soxhlet setup was employed for oil percentage determination that contains a round bottom flask of 250 ml, an exterior flask, and a reflex condenser by putting 5 gm of *Buxus papillosa* seeds powder in its thimble. 100 ml n-hexane was used as a solvent filled in the round bottle flask. The Soxhlet setup was run for 6 h at 60 °C (Ameen et al., 2023). During this process, the rotary evaporator has evaporated the superabundant solvent. At the end of this experiment, n-hexane was regained to ensure its reusability. The thimble containing seeds powder was taken from the Soxhlet setup and placed in the oven for 24 h at 65 °C to terminate the superfluous solvent and attain complete desiccation of the thimble (Alsaiari et al., 2022). Determination of oil content was carried out by thimble calculation using the following formula.

$$\text{Oil conc.}\% = \frac{(W_1 - W_2) - (W_3 - W_2)}{W_4}(100) \quad (1)$$

where, W_1 is the thimble plus seeds powder weight, W_2 equals to weight of evacuated thimble, W_3 equals to thimble weigh containing sample i.e., seeds powder after extraction process, and W_4 is the sample weight before extraction process. Seeds oil of *Buxus papillosa* has 45% oil concentration which makes it more potent, reliable and highly recommendable feedstock for biofuel production at industrial level.

2.3. Free fatty acids (FFA) calculation

The free fatty acidic concentration in filtered *Buxus papillosa* oil was calculated by acid-base titration procedure. Blank and sample titration was carried out successively by adding 0.025 M of potassium-hydroxide solution inside the burette and dripping it into a conical-shaped flask having 10 mL isopropanol and an indicator phenolphthalein (Munir et al., 2023). In sample titration 1 mL *Buxus papillosa* oil was used along with indicator. In sample titration 1 mL of *Buxus papillosa* oil was used along with an indicator. Readings of starting and final values were written down and both titrations were performed five times to calculate the average value (Rozina et al., 2022). The amount of FFA was found by using following equation (2)

$$(\text{FFAContent}) = \frac{\text{applied volume of sample titration} - \text{Volume utilized in blank titration}) x \text{MassofKOH used}}{\text{totalvolumeofoilused}} \quad (2)$$

2.4. Catalyst synthesis

Buxus papillosa fruit capsules as plant waste were utilized for preparing green bimetallic nanoparticles with sodium potassium tartrate for circular economy. In the previous literature, the *Buxus papillosa* fruit capsule was never used for nanoparticle synthesis. The fruit capsules were cleaned and washed with water to get rid of dust particles and other unwanted residues. 40 gm fruit capsules were taken in a 1 L beaker containing 500 ml distil water and heated at 250 °C on a hotplate for 5 h until the volume reduced to half. Filtration of the newly synthesized green aqueous extract was undertaken through funnel-fitted filter paper into the flask. The plant extract was kept in a refrigerator at 4 °C for 12 h.7.05 g of sodium potassium tartrate was mixed with 250 ml distilled water and dissolved by continuous stirring using magnetic stirrer for 30 min though the salt was readily water soluble. Thus 0.1 M solution was prepared. After that 250 ml of the prepared extract was mixed drop by drop using a pipette with the molar solution followed by continues stirring and heating at 50 °C for 2.5 h. Light brown colour liquid was poured into the petri plates and placed in oven at 60 °C to get complete desiccation. Scraper was utilized for scraping and transferring the dried catalyst into crucibles. 700 °C temperature was applied during calcination in a muffle furnace for 3.5 h. The Light brown colour catalyst was changed into black colour after calcination.

2.5. Transesterification through membrane reactor

The bimetallic green nanoparticles were applied and operated in a hydrophilic polymeric membrane reactor perform the process of transesterification with specific reaction conditions of time and thermal level, methanol ratio to oil and catalyst quantity loading along with known volume of *Buxus papillosa* seed oil. Interaction between targeted reacting components and membrane setup resulted in component's separation (Moyo et al., 2021). Circulation of methanol and glycerol through the membrane was due to their hydrogen bonding with the hydroxyl terminals of alcoholic polyvinyl. Membrane setup was kept with unprocessed chemical constituents and bio-diesel while constantly methanol and glycerolic residues were separated from the membrane. Four independently acting variables affecting the biodiesel output during transesterification were evaluated to ascertain the surpass conditions for transesterification (Soontarapa et al., 2023). The four evaluated variables include time in minutes (180), temperature (80 °C), oil to methanolic ratio (8:1) and catalyst amount loading (0.37 wt%).Yield percentage of bio-diesel and glycerol were evaluated with the yield percentage equation (Alsaiari et al., 2023b). The given equation (3) was used to calculate the yield percentage of methyl esters.

$$\text{Percentage of Yield} = \frac{\text{biodiesel gain in grams}}{\text{Crude oil utilize in grams}}(100) \quad (3)$$

2.6. Sodium potassium oxide green nano-catalyst characterization

Different innovatory tools i.e., FTIR, XRD, DRS, Zeta potential, SEM, EDS were taken into service for the characterization and analyzing the green novel bimetallic nano-catalyst and inquire its properties both chemical and physical (Abdullah et al., 2021). The crystalline structure along with size of particles, their symmetry, and crystal lattice configuration of sodium-potassium oxide nanoparticles were analysed by XRD Model JOEL JSM5910 applying CuK-α rays of wavelength 1.54 Å, 2° rate of scanning, 20 per min with range of scale 2θ = 5–70° (Kambo and Dutta, 2015). Surface morphological features of the novel bimetallic nano catalyst were anatomized through SEM while chemical

composition of nanoparticles was determined by Energy dispersive spectroscopy. The structural and functional groups constituents of sodium-potassium oxide nanoparticles were determined by FT-IR approach employing the range 4000–500 cm^{-1}.

2.7. Characterization of methyl esters

The chemical and physical properties of synthesized fatty acids methylated ester were determined via various analytical tools like Fourier Transform Infrared Spectroscopy, Nuclear Magnetic Resonance, and Gas chromatography-Mass spectroscopy. GC-MS techniques were employed in which Helium was applied as a gas carrier to investigate the composition of fatty acids methyl esters in the synthesized *Buxus papillosa* biodiesel (Siddiqi et al., 2020). A flow rate was fixed at 1.5 mL per minute with 220–370 °C column temperature. A spectrometer (Bruker) with a frequency 300 MHz was used to carry out NMR (^{1}H and ^{13}C) analysis of the biodiesel sample. 4000–400 cm^{-1} range of FT-IR with resolution 1 cm^{-1} and 15 cm^{-1} scans was employed to observe the functional group composition of *Buxus papillosa* seed crude oil and biodiesel.

2.8. Catalyst reusability

Nano-nature catalyst of the newly prepared bimetallic Phyto-nanocatalyst was taken into service during the process of transesterification within optimal values of molarity ratio between oil and alcohol (8:1), 80 °C thermal point, 0.37 wt% of catalyst concentration for 180 min duration of time. The nano-sized catalytic entities were centrifuged at 4500 rpm for 15 min. For the riddance of any impurity and attached polar and non-polar compounds from the catalytic nano-bodies, washing was done through water and n-hexane and kept inside the oven at 65 °C for 24 h (Alsaiari et al., 2023a). The procedure of calcination was performed at 700 °C for 3 h. Some of the nano-catalytic bodies were reused without second-time calcination during the process of transesterification to check the proper recycling-ability and efficacy (Ibrahim et al., 2022).

2.9. Experimental design and statistical findings

Different parameters are involved in the transesterification process of oil that leads to biodiesel formation. In this case, there are four variables i.e., A, B, C, and D representing the methanol ratio to oil, catalyst loading, time and temperature successively. These factors show an influential impact on the biodiesel yield in both ways independently and in a combined state. Central composite Design has been designed by the design of experiment having four variable factors with their minimum and maximum values such as A (8:1 to 20:1), B (0.1–0.37 wt%), C (80–130 °C), and D (60–180 min) as shown in Table 1. Analysis of variance was performed for checking the significance of these variable factors.

3. Results and discussion

3.1. BPO and FFA concentration

Novel waste, toxic and inedible of *Buxus papillosa* seeds oil was converted to environment remedial biodiesel. Previous literature exhorted that feedstock with oil content higher than 20% can only be employed for biofuel production. 45% seed oil content in the case of *Buxus papillosa* is a beneficial and highly vest candidate at a broader stage. Wild and vast distribution of *Buxus papillosa* further entrusts the commercialization purpose. The seed oil's free fatty acids concentration for BPBD was calculated before transesterification. FFA (0.25%) requires one-step transesterification as per past reports. Two-stepped transesterification applies to the feedstocks with FFAs concentration higher than 3% (Fadhil et al., 2020). The novel Phyto-nanocatalyst sodium/potassium oxide is prepared from novel salt sodium potassium tartrate and a novel fruit capsule aqueous extract of *Buxus papillosa* was recycled during transesterification for catalysis.

Table 1
Experimental design for transesterification reaction by central composite design.

Process parameters	−1	+1
Alcohol to oil ratio	8:1	20:1
Catalyst loading	0.1	0.37
Reaction time	60	180
Temperature	80	130

3.2. Characterization of Sodium–potassium oxide

Characterization of Sodium–Potassium oxide was done by different analytical tools. Detailed description of each analysis is given below.

3.2.1. X-ray diffraction findings of sodium-potassium oxide

Novel Phyto-nanocatalyst sodium/potassium oxide prepared from novel salt sodium potassium tartrate was further exposed for nano-size, crystalline nature, and hkl values (Miller indices). Cu-Ka rays having 0.154 nm wavelength were applied with the range of 5–70°and scanning rate of 2° per min. The observed peaks for Na/K oxide XRD were highly sharp that indicate a crystalline nature. Five main peaks for bimetallic Na/K oxide were noticed as having 2Θ values of 29.37, 32.98, 36.71,47.07,69.02, and corresponding Miller indices values (104), (110), (113), (116) and (217) calculated by Xpert High score software. Fig. 1a. illustrates the XRD graphic model for bimetallic Na/K oxide. The nano-bodies were checked for nano-size by Debye-Sherer's equation (Ingham, 2015). The average nano-size calculated for Na/K oxide was 23.5 nm. The resultant nano-size is within the high-performance range of 10 nm to 100 nm. Debye-Sherer's equation is as follows.

$$D = k\lambda/\beta\cos\theta \quad (4)$$

Here, 0.154 nm is the wavelength of X-rays represented by **λ** in the equation and FWHM (full width at half-maximum) is represented by **β**. The nano-size of the crystal nanocatalyst corresponds to **D**, and 0.94 is the **k** constant value.

3.2.2. Scanning electron microscopy (SEM) of bimetallic NPs

The micro-morphology of currently prepared Na/K oxide from *Buxus papillosa* fruit capsule aqueous extract has been evaluated by scanning electron microscopy. Scanned electron micrographs of magnification power 1 μm, 5 μm, and 10 μm for Na/K oxide are portrayed in Fig. 1b. Oval-shaped nanoparticles with sponge-like soft texture can be seen. Fluffiness and shape are the essential factors for proper catalysis and efficiency. The attractive forces between metals and oxide result in metallic bond formation and thus lead to agglomerated masses. There is a link between size variability and a higher ratio of surface and volume for Phyto-nanocatalyst. The catalysis efficiency of nanocatalysts depends on the presence of active sites (Buhr et al., 2009). More availability of active sites leads to a high rate of reaction and vice versa.

3.2.3. Energy dispersive X-ray spectroscopic analysis

The composition of different elements in bimetallic sodium-potassium oxide Phyto-nanocatalyst was determined through an energy-dispersive X-ray approach. Pure formation of nanoparticles and attachment of impurities can also be exploited by this technique (Dawood et al., 2022). Fig. 1c illustrates EDX graphic design for newly prepared bi-metallic sodium-potassium oxide with peak intensity on Y-axis and energy (keV) on X-axis. The oxygen element is at a peak (0.5 keV). Three peaks were noticed for potassium at 0.3, 3.3, and 3.6 (keV) while a single peak for sodium is present at 1.1 keV. A single peak for carbon is found at 0.1 keV that is due to organic plant extract. The

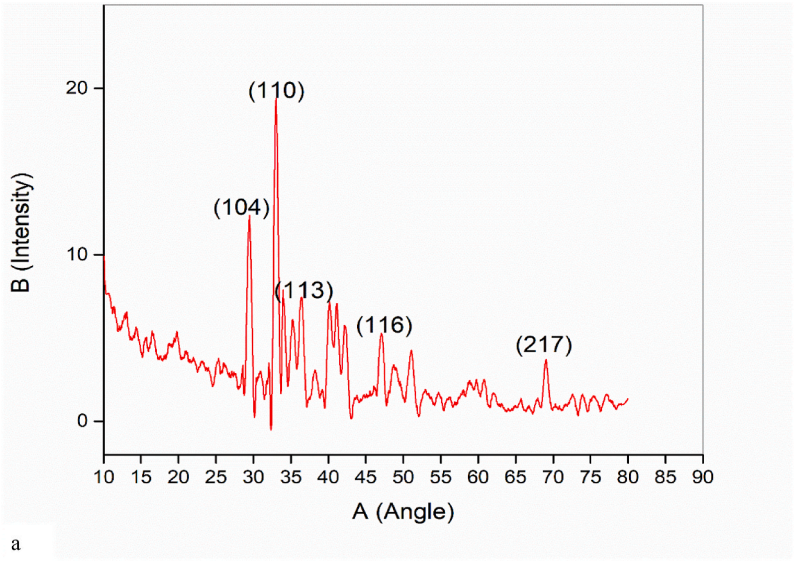

a

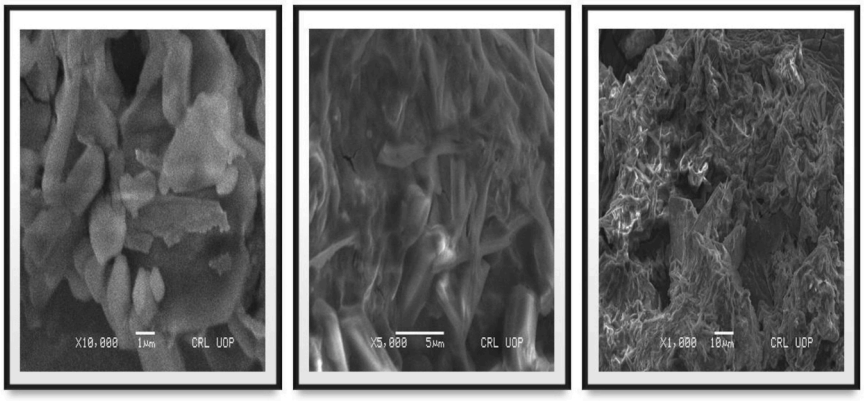

b

Fig. 1. a) XRD pattern of calcined Sodium Potassium oxide nano particles, **b** Scanning electron microscopy (SEM) of Sodium Potassium oxide NPs, **c)** Energy diffraction X-Ray (EDX) of Sodium Potassium oxide NPs**, d)** Spectral characteristics of Sodium Potassium oxide nano particles by diffuse-reflectance spectroscopy.

weightage percentage of each element was evaluated. The weight-percentages are 24%, 23.96%, 14.20% and 37.84% for carbon, oxygen, sodium and potassium in a successive manner. The atomic percentages of 39.33%, 29.47%, 22.16% and 19.84% are for carbon, oxygen, sodium and potassium successively.

3.2.4. *Diffuse reflectance spectroscopic outcomes*

Diffuse reflectance spectroscopic technique is applied to solid or powered form nanoparticles to evaluate their optical properties (Torrent and Barrón, 2008). The energy band gap for both crystalline and amorphous nature nano-objects is calculated by the DRS technique. The Kubelka-Munk function was applied to DRS-based data of bi-metallic sodium-potassium oxide and manipulated through Origin software (Landi et al., 2022). In this research, the band gap energy for newly prepared Na/K oxide turned out to be 3.42 eV represented by Fig. 1d.

3.2.5. *Zeta potential outcomes*

Zeta potential calculation is associated with electric charge strength in a liquified media. ZP measures the surface charge for nanocatalysts (Clogston and Patri, 2011). The calculation of the zeta potential for nano-catalysts used in bio-diesel preparation is important as it is a liquified medium. The strength, catalysis efficiency, and agglomerate formation of nanocatalysts are dependent on surface charge determination (Nayan et al., 2018). Zeta potential value for Na/K oxide turned out to be −13.3 mV. This ZP value indicates a negative charge on the surface of the nanocatalysts. These newly prepared Na/K oxide nanoparticles are stable enough as the good stability range is between ±10 to ±30 mV. The graphical presentation of surface charge is mentioned in Fig. 2a.

3.2.6. *FT-IR spectroscopic outcomes*

The newly synthesized Phyto-nanocatalyst sodium-potassium oxide's composition of functional groups variability was determined through the FT-IR. A frequency range of 500–4000 cm^{-1} was applied to Na/K oxide during the analysis. The formation of Phyto-nanocatalyst is validated by peaks in the range of 500–600 cm^{-1} that are due to the metallic bonding of potassium with oxygen. A sharp and strong peak at 883.23 cm^{-1} is due to the presence of sodium -oxygen bonding as shown in Fig. 2b. The other observed functional groups are alkyl halides (500 -600 cm^{-1}), C–C stretching (1406.13 cm^{-1}), C═O (1749.11 cm^{-1}), and alcoholic and phenolic and water absorbance is represented by a broad peak 3401.81 cm^{-1}(OH) group.

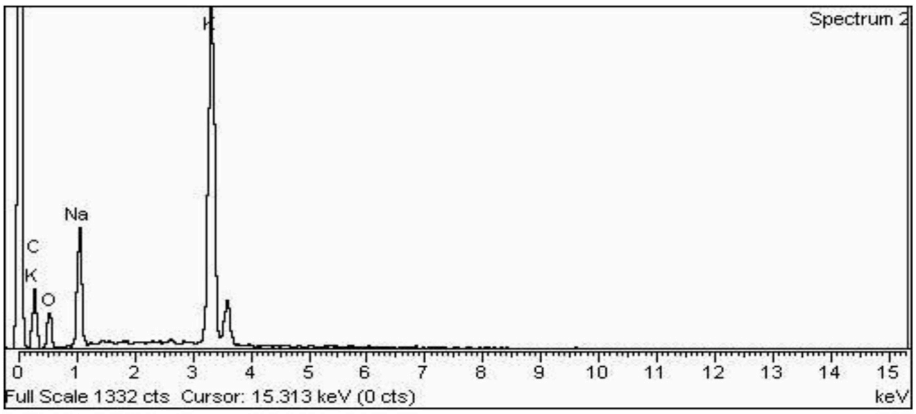

c

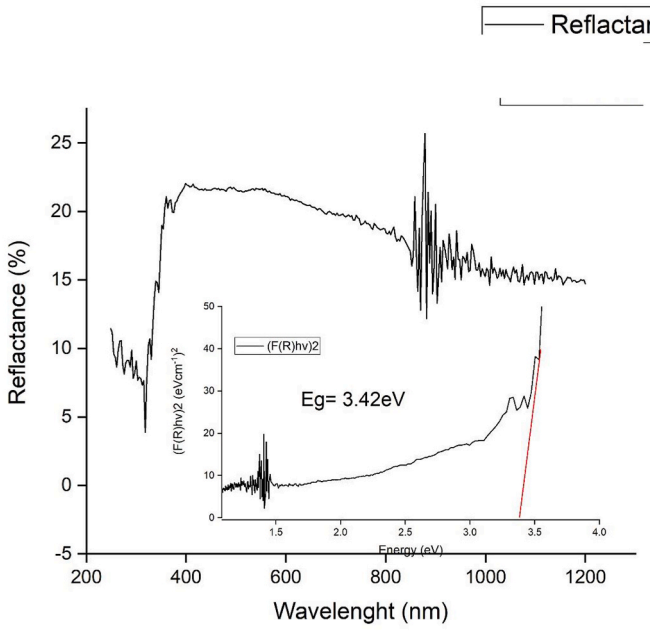

d

Fig. 1. (*continued*).

3.3. Application of response surface methodology for Buxus papillosa biodiesel optimization

Different parameters are involved in the transesterification process of oil that leads to biodiesel formation. In this case, there are four variables i.e., A, B, C, and D representing the methanol ratio to oil, catalyst loading, temperature, and time successively (Bhatia et al., 2021). These factors show an influential impact on the biodiesel yield in both ways independently and in a combined state. Central composite Design has been designed by the design of experiment having four variable factors with their minimum and maximum values such as A (8:1 to 20:1), B (0.1–0.37 wt%), C (80–130 °C), and D (60–180 min) as given in Table 2.

R^2 = 0.8371, Std. Dev = 7.54, C.V. % = 10.52, Adeq Precision = 7.2712.

The yield predicted by the experimental design and the experimentally obtained yield during transesterification are compared in Fig. 3a. The predicted and experimentally obtained yields are approaching the straight line in the graph as the variables show correlated influence. ANOVA (Analysis of variance) for the current data is mentioned in Table 2. A quadratic model was utilized and prepared through response surface methodology (Borah et al., 2019). The model turned out to a significant having 0.0013 p-value. The lack of fit for the experimental model is not significant in comparison with pure error as F-value is 1.75 and the p-value is 0.2793. Non-significant value for lack of fit is in the favour of quadratic model having a 27.93% chance can occur by noise. A^2 (Methanol to oil ratio) is the highly significant quadratic term with p-value of 0.0021 as smaller than 0.05 while the p-values for B^2, C^2 and D^2 are 0.0107, 0.0071, and 0.0227 in a successive way. 0.8918 is the adjusted value of R^2 and the predicted value of R^2 is 0.7594 and has a variation less than 0.2. The adequate precision value of the quadratic model is 7.2712 which is higher than 4. This value of adequate precision advocates the model to obtain a higher yield of biodiesel. The calculated yield polynomial equation of biodiesel is mentioned as follow.

$$\text{BPBD yield} = (+71.45) + (-6.61*A) + (+5.10*B) + (-5.38*C) + (+2.29*D) + (-0.2320*AB) + (+3.38*AC) + (-0.1250*AD) + (-2.13*BC) + (+0.4817*BD) + (+0.7500*CD) + (-3.23*A^2) + (-0.0151*B^2) + (+3.60*C^2) + (-1.12*D^2) \quad (5)$$

3.4. Reaction parametric influence on transesterification

The interaction of four varying factors during the process of transesterification is denoted by 3-dimensional graphic models as demonstrated in Fig. 3b. By these surface response graphic models, the optimum values for each factor can be achieved. There is a certain optimal value for each factor at which the yield is maximum but there is

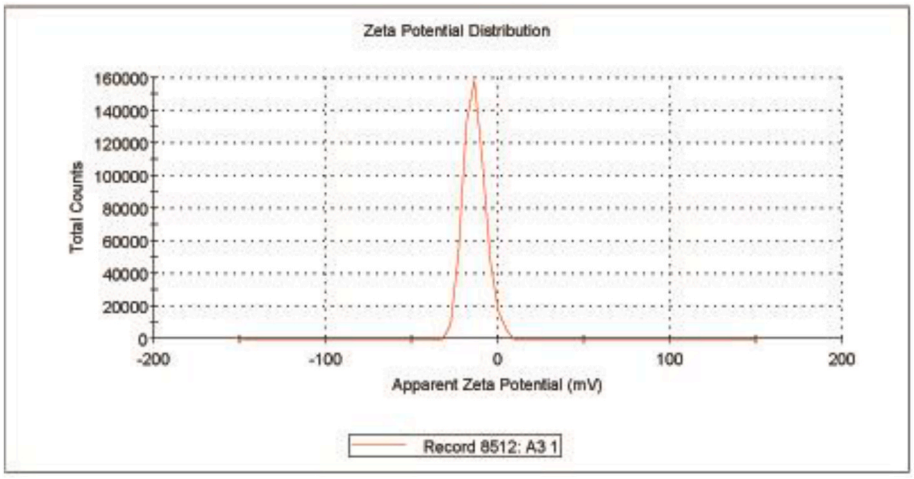

a

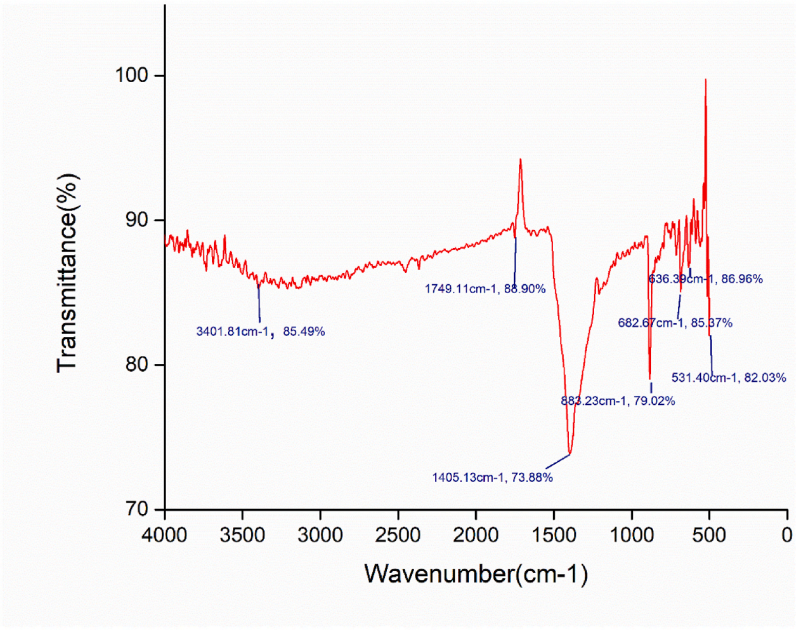

b

Fig. 2. a) Zeta potential measurement of Sodium Potassium oxide nano particles, b) FTIR spectrum of Sodium Potassium oxide nano particles.

reduction in yield with the decrement and increment values for these factors beyond the optimum (Chaudhry et al., 2022).

3.4.1. *Correlative influence of methanol ratio to oil and catalyst amount*

Biodiesel yield is highly affected by catalyst amount and methanol ratio to oil during transesterification. The correlative influence of methanolic ratio to oil and catalyst quantity on *Buxus papillosa* biodiesel yield is portrayed in Fig. 3b1. Highest yield of 97% was secured during run 19 at optimal reaction conditions of molar ratio (8:1), catalyst quantity (0.37 wt%), temperature (80 °C), and time of 180 min. A gradual diminution in yield can be seen in the varied reaction conditions. The influence of molar ratio and catalyst used amount was visualized by keeping the other two factors constant at 80 °C temperature and 180 min time duration. A yield diminution of 13% occurred in run 12 at a molar ratio of 8:1 and 0.1 wt% of catalyst quantity. A minimum quantity of catalyst does not have enough active sites for the complete conversion of oil into biodiesel (Dawood et al., 2021). A diminished yield of 79% was secured in round 29 at the highest molar ratio of 20:1 and 0.37 wt% catalyst quantity. Transesterification moves in both directions i.e., forward, and backward. Excessive availability of methanol leads to catalyst dilution and thus turns the reaction in a backward direction that enables glycerol and fatty acids methyl esters to react and form mono-glycerides (Dubé et al., 2007). The correlative influences of catalyst quantity and methanol oil molar ratio proved to be significant as the p-value is 0.0037 (smaller than 0.05). Solely, molar ratio and catalyst are significant with p-values of 0.0021 and 0.0107 successively.

3.4.2. *Correlative influence of methanol ratio to oil and temperature*

Fig. 3b2 is representing the combined influence of temperature and the molar ratio of oil and methanol. Values for catalyst amount and time were fixed at 0.37 wt% and 180 min successively while evaluating the correlative influence of molar ratio and temperature on BP biodiesel yield. The highest yield for *Buxus papillosa* biodiesel was 97% secured during round 19 at 80 °C thermal setup and molar ratio (8:1). Heating at

Table 2
ANOVA for Response Surface Quadratic model.

Source	Sum of Squares	df	Mean Square	F-value	p-value	
Model	2391.44	14	170.82	3.00	0.0013	significant
A-Methanol to oil ratio	786.93	1	786.93	13.84	0.0021	
B-Catalyst loading	482.42	1	482.42	8.48	0.0107	
C-Temperature	552.39	1	552.39	9.72	0.0071	
D-Time	92.02	1	92.02	1.62	0.0227	
AB	0.8610	1	0.8610	0.0151	0.0037	
AC	182.25	1	182.25	3.21	0.0436	
AD	0.2500	1	0.2500	0.0044	0.0480	
BC	72.57	1	72.57	1.28	0.0263	
BD	3.83	1	3.83	0.0674	0.0486	
CD	9.00	1	9.00	0.1583	0.0163	
A^2	31.35	1	31.35	0.5514	0.0092	
B^2	0.0006	1	0.0006	9.796E-06	0.0375	
C^2	51.15	1	51.15	0.8997	0.0579	
D^2	2.51	1	2.51	0.0441	0.0365	
Residual	852.86	15	56.86			
Lack of Fit	663.19	10	66.32	1.75	0.2793	not significant
Pure Error	189.67	5	37.93			
Cor Total	3244.30	29				

Table 3
FTIR spectrum of *Buxus papillosa* biodiesel.

S. no	Frequency (cm^{-1})	Absorbances (%)	Vibration Types	Functional Groups
1	3008.36	0.02	= CH stretching	Alkene
2	2922.72	0.19	CH_2 stretching	Alkene
3	2853.38	0.13	CH_3 stretching	Alkane
4	1741.47	0.26	C═O stretching	Ester
5	1463.96	0.08	O–CH_3 typical	Methyl ester group, Alkane
6	1435.49	0.09	O–CH_3 typical	Methyl ester group, Alkane
7	1365.08	0.04	CH_3 adjacent to C═C	Methyl group, Alkene
8	1243.93	0.08	C–CO–O	Ester
9	1169.28	0.15	C–O–C stretching	Aliphatic ester
10	1195.36	0.12	C–O/O–CH_3 stretching	Ester
11	1019.91	0.04	C–O–C stretching	Ester
12	722.19	0.09	-C═CH_2	Olefin carbon

Table 4
NMR spectroscopy of *Buxus papillosa* biodiesel.

1H Protons	Functional groups	Chemical shift (ppm)	Peak splitting
CH_3-C	Terminal methyl group	0.832–0.887	Sextet
-(CH_2)n-	Backbone CH_2	1.232–1.352	Quadruplet
-CH_2-CH_2-COOH	Beta-methylene group	1.573–1.617	Triplet
= CH–CH_2-	Alpha- methylene group attached with one double bond	1.975–2.057	Quintet
CH_2COOR	Alpha-methylene group attached with ester	2.250–2.302	Triplet
= CH–CH_2-CH =	Alpha- methylene group attached with two double bonds	2.727–2.764	Triplet
-$COOCH_3$	Methyl group of esters	3.635	Singlet
-CH═CH-	Olefinic protons	5.276–5.362	Septet
13C protons	**Functional groups**	**Chemical shift (ppm)**	**Peak splitting**
-COO-	Carbonyl carbon of ester	174.19	Singlet
-CH═CH-	Inner non-conjugated carbons, unsaturation in fatty acids methyl esters	127.84–127.97	Doublet
CH═CH-	Outer non-conjugated carbons, unsaturation in fatty acids methyl esters	129.64–130.07	Triplet
-C-O	Carbonyl carbon of ester	76.67–77.52	Triplet
-C-O	Methoxy carbon of ester	51.31–51.35	Doublet
(-CH_2-)n	Methylene carbons of carbon chain in methyl esters	24.90–34.03	Multiple

80 °C provides enough KE (kinetic energy) to the reacting mixture for final product formation. Run 30 resulted in a 72% BPBD yield when a maximum limit of temperature and molar ratio was applied i.e., methanol: oil (20:1) and temperature 130 °C. This yield diminution is due to the saponification reaction and limited boiling point of methanol (Endalew et al., 2011). A higher molar ratio also lessens the yield by diluting the catalyst which leads to glycerolises. Run 24 gave an 80% yield at a molar ratio (14:1) and temperature of 105 °C. Decreasing both coordinated factors here results in yield uprising compared to run 30. The experimental work has also proved the correlation between these factors. The ANOVA-based outputs for these coordinated factors are significant in an associated state as well as in individual form having p-values smaller than 0.05.

3.4.3. Correlative influence of methanol ratio to oil with the time factor

Fig. 3b3 portrays the correlative influence of the methanol ratio to oil with the time factor on BPBD's yield in three-dimensional graphic form. The coordinated impact of reaction duration and alcohol-to-oil ratio was checked at a fixed catalyst quantity (0.37 wt %) and thermal setup of 80 °C. Round 19 ended with the highest yield of 97% in a duration of 180 min at a molar ratio (8:1). Run 8 ended with an 86% yield when the time was reduced to 1 h. Run 22 ended with a 74% yield at 20:1 (alcohol: oil) and a minimum time of 60 min. A shorter duration of time usually results in a lower yield as the reactant cannot react completely to form the final biodiesel yield (Gómez-Trejo-López et al., 2022). Round 29 ended with a biodiesel output of 79% at molar ratio of 20:1 and ideal time duration of 180 min. The output diminution in this case is due to an increased amount of alcohol. The investigative study and ANOVA results for the correlative influence of methanol ratio to oil with the time factor proved that these parametric factors have significances with the p-value (0.0436) while both these factors are significant as a singly acting variables with p-values smaller than 0.05 (mentioned in Table 2).

3.4.4. Correlative influence of catalyst amount with temperature

Coordinated impact of catalyst amount with temperature is illustrated in a 3-dimensional graphic model in Fig. 3b4. The coordinated impact of catalyst amount with temperature was studied at constant methanolic ratio to oil (8:1) and duration of 180 min. Round 19 resulted in the highest yield of 97% at 80 °C and 0.37 wt% of catalyst quantity.

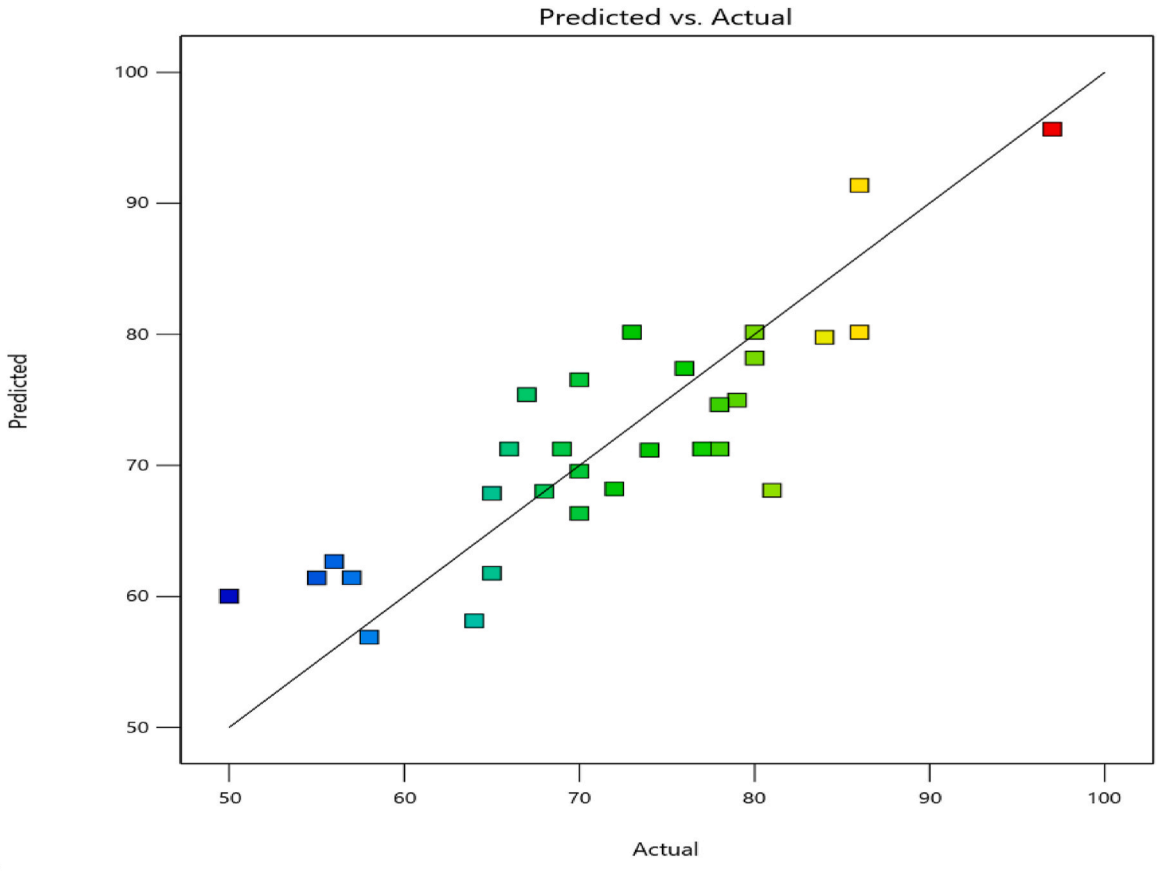

Fig. 3. a) Comparison between the experimental biodiesel yield and predicted yield of the model, **b)** Right and left plots showing parametric impact on yield of biodiesel (b1) Methanol to oil molar ratio and catalyst loading (b2) Methanol to oil molar ratio and reaction time (b3) Methanol to oil molar ratio and temperature (b4) Catalyst loading and reaction time (b5) Catalyst loading and temperature (56) Reaction time and temperature

Round 13 ended in 68% yield of biodiesel with decreased quantity of catalyst (0.1 wt%) and enhanced temperature 130 °C. A diminished yield of 84% was noted in round 12 at 0.1 wt% quantity of catalyst and thermal point of 80 °C. Such decrease in yield is linked with enhanced temperature that influence the methanol's boiling point and minimal quantity of catalyst (Abdelmigeed et al., 2021). The coordinated impact of catalyst amount with temperature has shown significance with collective p-value equals to 0.0263 while these independently acting factors significant as catalyst amount has p value (0.0107), and temperature has p value (0.0071) as given ANOVA Table 2.

3.4.5. *Correlative influence of catalyst amount with reaction time*

Coordinated impact of catalyst amount with reaction duration is illustrated in a 3-dimensional graphic model as shown in Fig. 3b5. The coordinated impact of catalyst amount with reaction duration was studied at constant methanolic ratio to oil (8:1) and temperature of 80 °C. Round 19 ended with a maximum yield of 97% at optimized limits of 0.37 wt% (catalyst amount) and 180 min (time). Round one ended with 76% biodiesel's yield at minimal quantity of catalyst (0.1 wt%) and 60 min duration of time. During round 12 when duration was increased from 60 min to 180 min while rest of the conditions were same as round 1, the yield increased to 84%. The overall diminution in yield is associated with lesser time for the reacting components that leads to incomplete conversion of triglycerides into fatty acids methyl esters and a minimal quantity of catalyst that does not provide adequate active sites for catalysis (Ahmad et al., 2022a). Analysis of variance-based results for the coordinated impact of catalyst amount with reaction duration was found significant with p-value equals to 0.0486 while singularly catalyst quantity (p-value = 0.0107) and time (p value = 0.0227) are significant.

3.4.6. *Correlative influence of reaction temperature along with time*

The correlative influence of reaction temperature along with time on *Buxus papillosa* biodiesel's yield is given in Fig. 3b6. The investigation for coordinated impact of reaction temperature along with time factor was done under constant molar ration (8:1) and nano-catalyst amount (0.37). A temperature of 80 °C and time duration of 180 min resulted in maximal yield of 97% during round 19. By increasing the temperature up to 130 °C for short duration of 60 min in round 7 ended with 81% yield. A further decrease in yield (67%) occurred when the reaction was run for 180 min at 130 °C. This diminution of yield is associated with the limitation of methanol boiling point. Increased temperature results in good yield up to an optimized level beyond that point further increment of temperature diminished the reaction rate in forward direction (Borah et al., 2019). ANOVA resultant data testify the significance of correlative influence of reaction temperature and time with 0.0163 (p value). Both factors are significant singularly with p values 0.0071 and 0.0227 successively for temperature and time.

3.5. *Biodiesel characterization*

3.5.1. *FTIR analytical findings*

The Fourier transformed-infrared spectroscopic characterization of BPBD and BPO in the range 515–4000 cm^{-1} is represented by Fig. 4. Table 3 enlists the main observed functional groups with corresponding frequency, absorbance, and vibrational type in BPBD sample. The successful transformation of oil into diesel is confirmed by two characteristic peaks at 1741.47 cm^{-1} (C═O) and 1435.49 cm^{-1} (O–CH3).

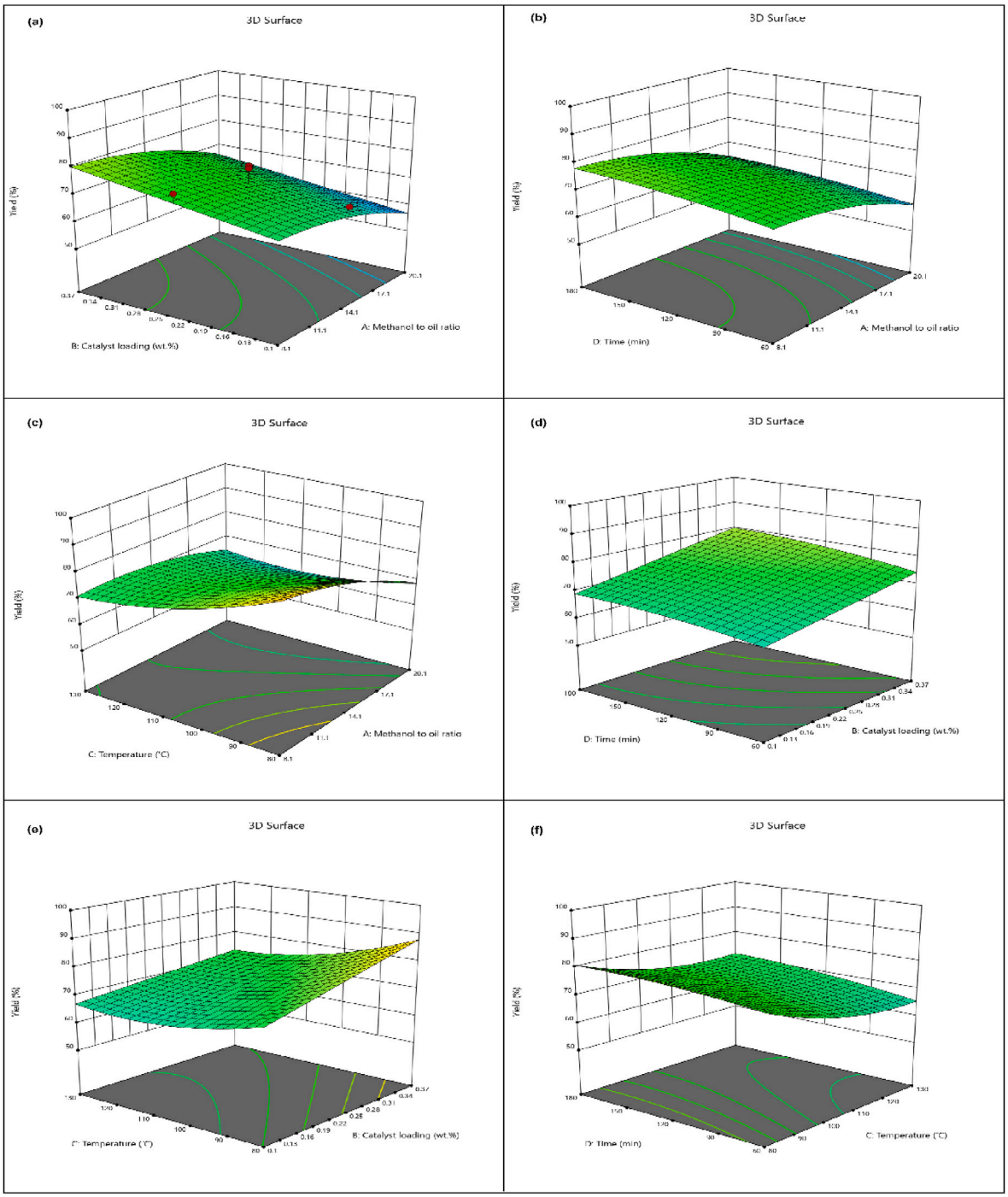

b

Fig. 3. (*continued*).

The BPO FTIR mainly differs from BPBD in the intensities of absorbance. The main bands in the oil spectrum are 2922.35 cm^{-1} (CH_2 stretching, alkene), 2853.01 cm^{-1}(C–H stretch of sp^3 hybridization), and 1743.19 cm^{-1} is associated with C═O stretch, 1464.83 cm-1 for CH_2 bend, 1377.70 cm^{-1} is for CH_3 bending and 1160.20 cm^{-1} (sp^3, alkane C–H bends). A band at 3330.29 cm^{-1} represents the hydroxyl group in *Buxus papillosa* oil which is absent in the BPBD FTIR spectrum. A peak of 1160.20 cm^{-1} in the BPO spectrum is divided into two separate peaks 1169.28 cm^{-1} and 1195.36 cm^{-1} in the biodiesel FT-IR spectrum.

3.5.2. NMR spectroscopic analysis

A nuclear magnetic resonance tool was applied to BPBD prepared sample to gain confirmation about chemical constituents. The affirmation of fruitful conversion of tri-glycerides into diesel is massively done by ^1H and ^{13}C NMR (Diehl and Randel, 2007). Table 4 contains the resultant data of ^1H NMR and ^{13}C NMR for *Buxus papillosa* biodiesel. ^1H and ^{13}C protons along with their corresponding functional groups, chemical shifts (ppm), and peak splitting are mentioned in Table 4.

The main band in ^1H NMR at 3.635 ppm (methyl group of esters) confirms biodiesel formation. Carbonyl carbon of ester at 174.19 ppm in ^{13}C NMR is another confirmation for biodiesel formation. The graphical

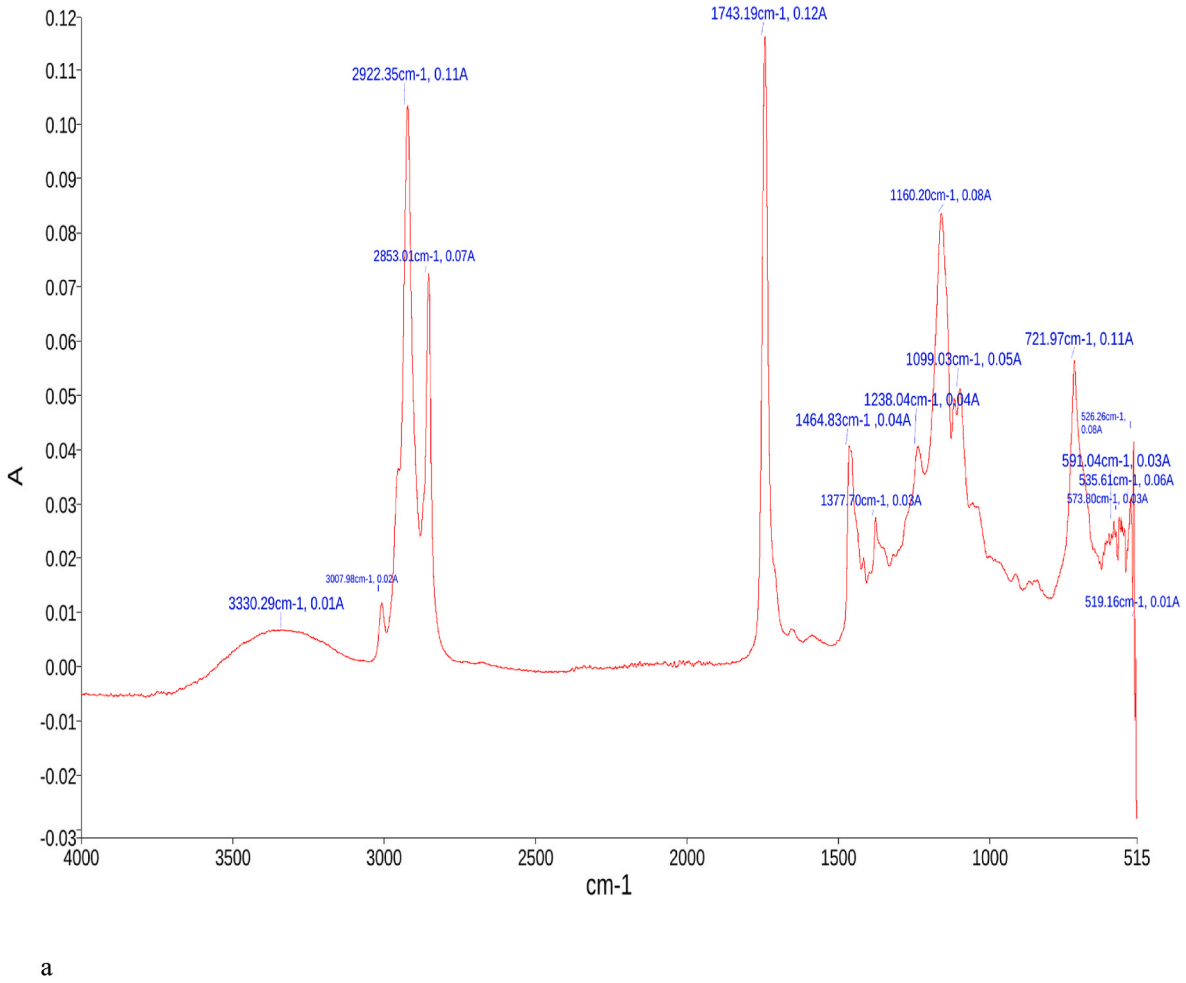

Fig. 4. FTIR spectrum of **(a)** seed oil of *Buxus papillosa* (b) *Buxus papillosa* Biodiesel.

representation of both ^{1}H NMR and ^{13}C NMR is given in Fig. 5 **(a)** and **(b)** respectively. All observed spikes agree with the previous work (Ahmad et al., 2022a). The percentage conversion of triglycerides in oil to methyl-esters has been calculated by a formula below, it turned out to be 97%.

$$C = 100.\frac{2AMe}{3ACH_2} \quad (6)$$

here, C = percentage transfiguration of tri-glyceride to bio-diesel, AMe = integration data of proton for methoxy group while ACH_2 represents the value of integration of alpha-methylene proton integration in BPBD.

3.5.3. GC/MS analysis

The chemical composition of bio-diesel is dependent on feedstock source. In the current research, the prepared *Buxus papillosa* bio-diesel sample was gone through GC/MS tool for analytical findings of fatty acid methyl esters. Table 5 enlists the GC/MS library match results of BPBD. Fig. 6 represents the GC/MS peaks observed for BPBD sample.

The GM/MS findings of BPBD sample show a total of seventeen methyl esters. 9-Octadecanoic acid methyl ester (C18:1) is key methyl ester fatty acid in BPBD sample at retention time 18.787 min (**Table 5**). Five compounds are unsaturated in which four are mono-unsaturated while one is di-unsaturated. The rest of the twelve compounds are saturated in nature. As the results show a lower ratio of unsaturated methyl esters, *Buxus papillosa* bio-diesel has a good property of fuel-efficient combustion and is recommendable for practical application in engines (Koria and Nithya, 2012). *Buxus papillosa* seeds oil has a proficient capability for biodiesel conversion as per GC/MS results.

3.6. Fuel characteristics of BPBD

Before introducing a novel source of biodiesel to the market, different properties of fuel must be known. Fuel characteristics provide information about fuel performance in the engine, transportation, storing safety, and the impact of fuel on the environment (Lin et al., 2006). In this research, *Buxus papillosa* bio-diesel has been evaluated for fuel properties determination as shown in Table 6.

The resultant data was matched with internationally implemented fuel limitations like that of American, Chinese, and European standards. Previously done research also supports our currently conducted study.

3.6.1. Acid number

The total acidic value for biodiesel is the number of total FFAs that usually cause corrosion to the engine (Wang et al., 2008). It is calculated by the amount of KOH used for the neutralization of 1 g of bio-diesel. The engine is subjected to corrosion if biodiesel has a high acidic value. In the currently conducted research, the acidic value of *Buxus papillosa* seed oil-based bio-diesel (0.32 mg KOH/g) is matched with international limitations.

3.6.2. Kinematic viscosity

The kinematic viscosity affects the atomization and formation of deposits inside the engine. Engine deposition occurs when viscosity is

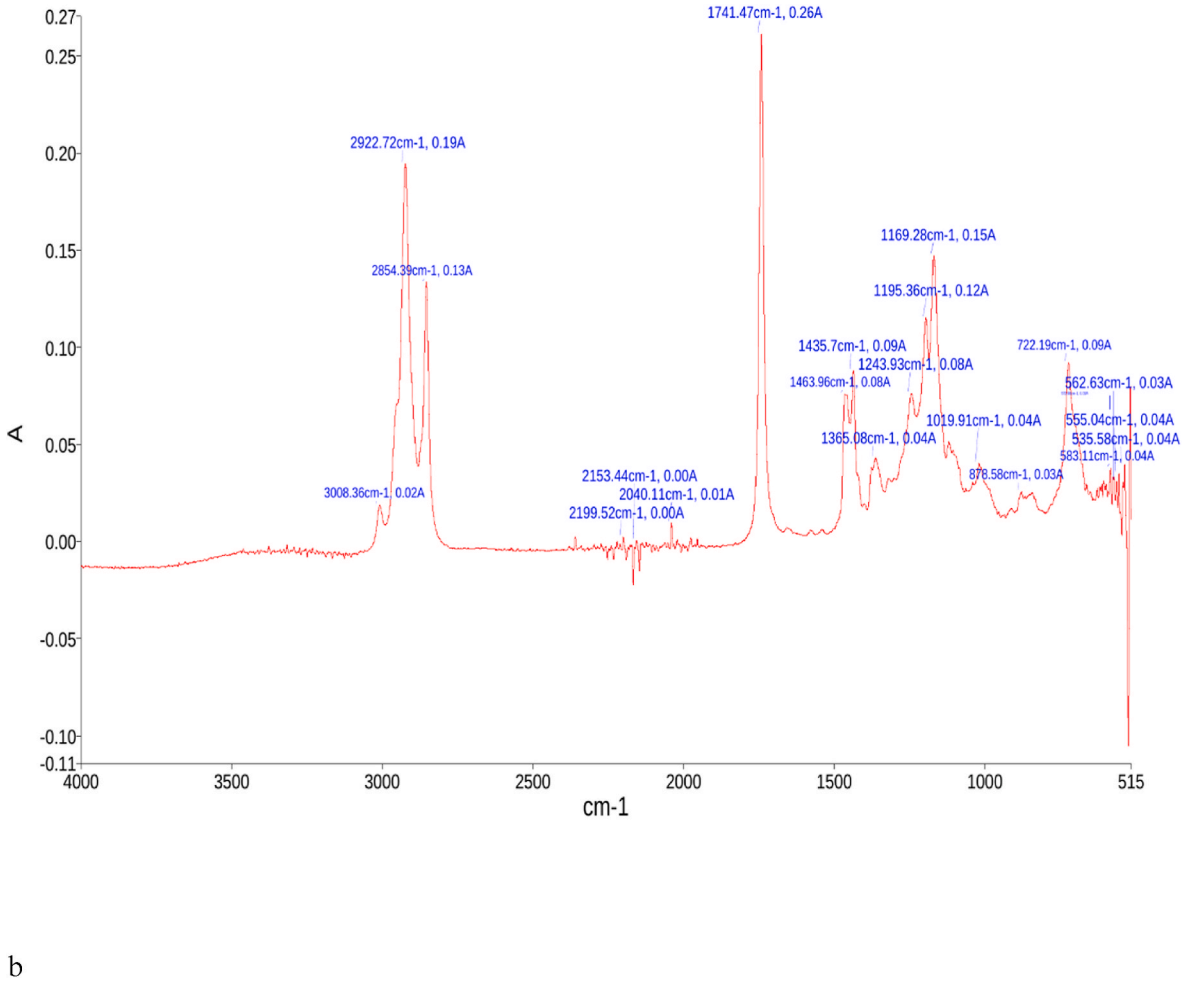

Fig. 4. (*continued*).

relatively more than the internationally set limits and thus causes deposition (Knothe and Steidley, 2005). A lower value for the viscosity is favorable for engine lifetime and performance. In the currently conducted research, the kinematic viscosity of *Buxus papillosa* seed oil-based bio-diesel (5.01 mm^2/s) is comparable with international limits. According to previously done research, the kinematic viscosity of biodiesel elevates with the passage of time during storing.

3.6.3. Fuel density

Fuel density has an impact on the combustion and injection process into the engine at lower temperatures (Ramírez Verduzco, 2013). Viscosity and stickiness issues of fuels are also concerned with higher values of density (Nabipour et al., 2020). Past work revealed that petro-diesel has smaller densities than synthesized bio-diesel (Ahmad et al., 2022b). In the currently conducted research, the fuel density of *Buxus papillosa* seed oil-based bio-diesel (0.89 kg/m^3) is according to international limitations.

3.6.4. Pour point

The pour point of a fuel is the limit of temperature where biodiesel can flow freely and beyond that limit, it resists flow due to thickness. The pour point has a noticeable impact on biodiesel during winter at lower temperatures (Wang et al., 2012). In the currently conducted research, the pour point of BPBD (−9 °C) is comparable with international limits.

3.6.5. Cloud point

The cloud point of bio-diesel is the limit of temperature beyond which crystal formation starts. Engine efficacy and fuel performance during freezing temperatures are highly influenced by the cloud point (Yaşar, 2020). The cloud point of BPBD is −8 °C which is under the limitation of international standards.

3.6.6. Flash point

The flash point of bio-diesel is a point of temperature where ignition may occur. It is an essential fuel property regarding the commercialization and safety of transportation and storage (Santos et al., 2020). The flash point of the currently prepared *Buxus papillosa* seed oil-based bio-diesel sample is 75 °C which lies within the internationally set limits for fuel and is best for commercialization purposes.

3.6.7. Sulphur content

Fuel's sulphur emission percentage is a highly concerned property of biodiesel regarding environmental safety and healing. Preference for commercialization is linked with a lower sulphur emission percentage (Samuel et al., 2019). The sulphur emission percentage for *Buxus papillosa* biodiesel is 0.0009 which is lesser than 1 ppm. In comparison petroleum diesel has a 50-ppm sulphur emission percentage which is far more than this currently conducted study. Dealing with environmental toxicology, its remediation and circular economy, novel *Buxus papillosa* toxic seeds oil conversion to non-hazardous and eco-healing biodiesel can prove an efficient entrant in biofuel industry.

3.7. Catalyst reusability

Reusability of heterogenous nano catalyst is one of the beneficial points over conventional homogenous catalyst. In present experimental

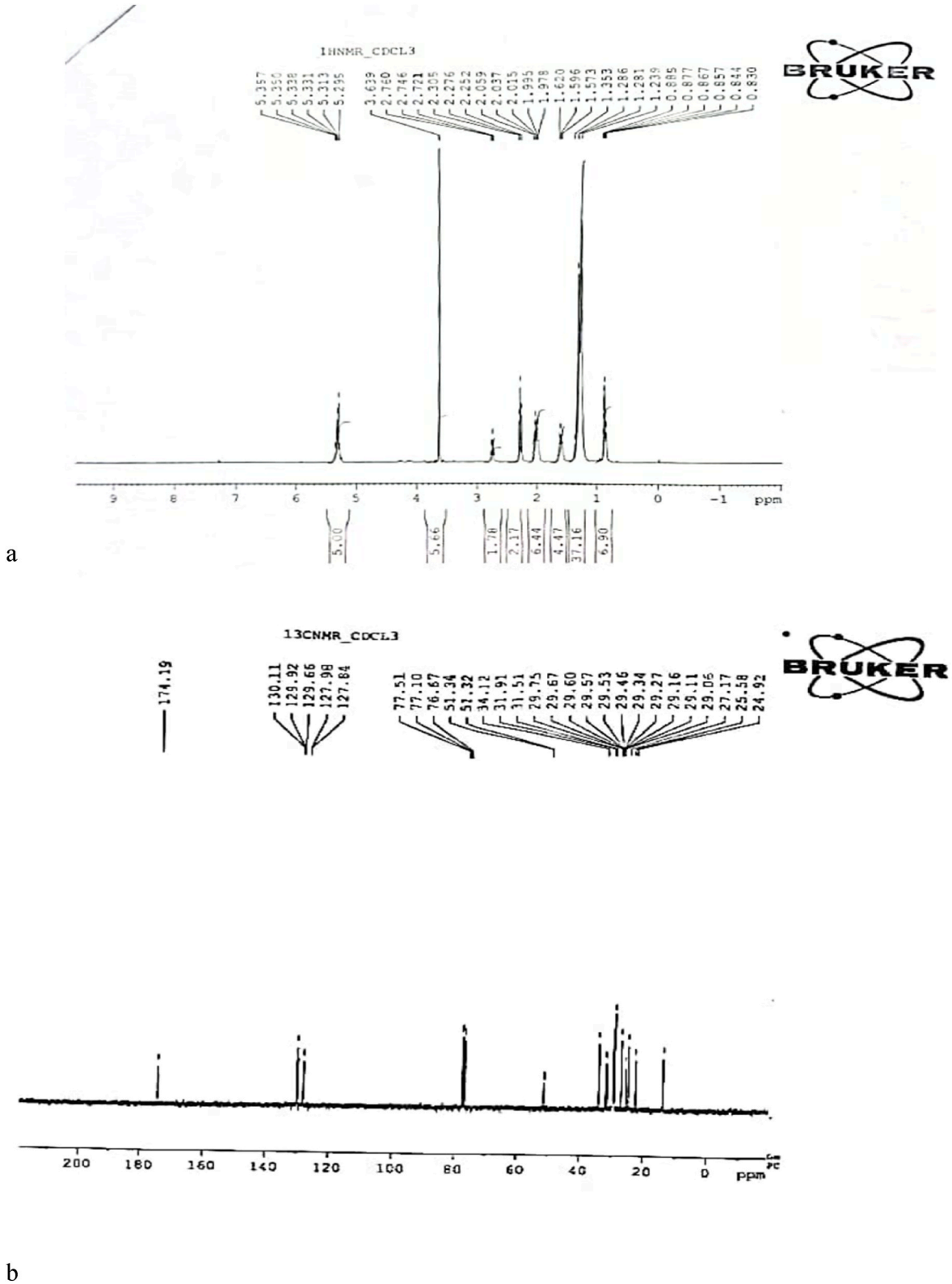

Fig. 5. NMR spectrum of *Buxus papillosa* biodiesel **(a)** ^{1}HNMR and **(b)** ^{13}CNMR.

work reusability of heterogenous green bimetallic NPs is tested under standard experimental conditions of transesterification such as methanol to oil molar ratio of 8:1, reaction time (180 min), temperature (80 °C) and catalyst loading (0.37 wt%), After each transesterification reaction reusability of nano catalyst has been measured. After separation from reaction mixture catalyst has been washed with water and n-hexane to remove any remaining glycerol or biodiesel (Abdelmigeed et al., 2021). Recalcination at 700 °C for 3 h was applied to recover the catalytic ability of the phyto-nanocatalyst. Experimental data uncovered that bi-metallic sodium/potassium oxide Phyto-nano catalyst can be reused effectively in three successive cycles because there is no or little notified change in biodiesel yield. In fourth, fifth and sixth experimental

Table 5
GC/MS Analysis of *Buxus papillosa* biodiesel.

No.	Identified Compounds	Retention Time (min)	Molecular Formula	Corresponding Acid	Compound Type
1	Octanoic acid, methyl ester	6.924	$C_9H_{18}O_2$	C8:0	Saturated
2	Decanoic acid methyl ester	10.005	$C_{11}H_{22}O_2$	C10:0	Saturated
3	Undecanoic acid 10-methyl, methyl ester	12.648	$C_{13}H_{26}O_2$	C11:0	Saturated
4	Dodecanoic acid, methyl-esters	12.648	$C_{13}H_{26}O_2$	C12:0	Saturated
5	Methyl tetra decanoate	14.939	$C_{15}H_{30}O_2$	C14:0	Saturated
6	6- pentadecanoic acid 13-methyl, methyl ester	16.769	$C_{17}H_{34}O_2$	C15:0	Saturated
7	9-Hexadecenoic acid, methyl esters	16.769	$C_{16}H_{30}O_2$	C15:1	Mono-unsaturated
8	Hexadecenoic acid, methyl ester	17.062	$C_{17}H_{34}O_2$	C16:0	Saturated
9	Pentadecanoic acid 14-Methyl, methyl ester	17.062	$C_{17}H_{34}O_2$	C15:0	Saturated
10	9, 12 Octadecadienoic acid methyl ester	18.700	$C_{19}H_{34}O_2$	C18:2	Di-unsaturated
11	9-Octadecanoic acid methyl esters	18.787	$C_{19}H_{36}O_2$	C18:1	Mono-unsaturated
12	Methyl Stearate	18.965	$C_{19}H_{38}O_2$	C18:0	Saturated
13	Cis-methyl 11-eicosenate	20.401	$C_{21}H_{40}O_2$	C20:1	Mono-unsaturated
14	Cis-13 Eicosanoid acid, methylate-ester	20.401	$C_{21}H_{40}O_2$	C20:1	Mono-unsaturated
15	Eicosanoid acid, methyl ester	20.642	$C_{21}H_{42}O_2$	C20:0	Saturated
16	Methyl-18-methyl nonadeconoate	22.196	$C_{21}H_{42}O_2$	C19:0	Saturated
17	1,2-Cyclohexane di-carboxylic acid decyl methyl ester	22.669	$C_{19}H_{34}O_4$	C18:0	Saturated

Table 6
Fuel properties of *Buxus papillosa*.

Property	Methods	Results	ASTM Standard	ASTM D-6751	EN-14214	China GB/T 20828–2007
Color	Visual	2	2.0	2.0	_	_
Acid number (mg KOH/g)	ASTM D-974	0.32	≤0.5	≤0.5	≤0.8	≤0.5
Flash Point (°C)	ASTM D-93	75	60–100	≥93	≥130	≥120
Pour Point (°C)	ASTM D-97	−9	−15–16	−15–16	_	_
Viscosity (mm2/s at 40)	ASTM D-445	5.01	1.9–6.0	1.9–6.0	_	3.4–5.0
Density (kg/m3 at 40 °C)	ASTM D-1298	0.89	0.86-0.90	≤120	_	≤120
Sulphur content (wt. %)	ASTM D-4294	0.0009	0.05	≤0.05	≤0.05	≤0.20
Cloud point (°C)	ASTM D-2500	−8	−3.0–12	3.0–12	_	_

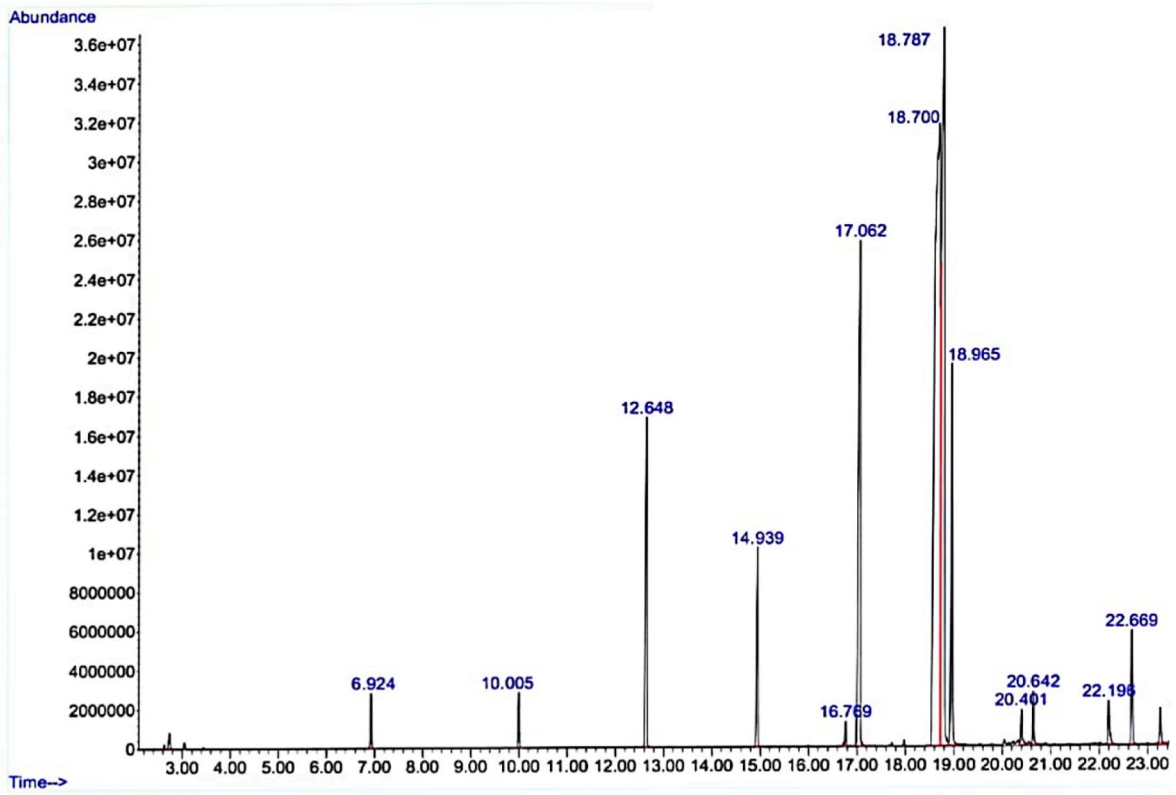

Fig. 6. GC-MS spectrum of *Buxus papillosa* biodiesel.

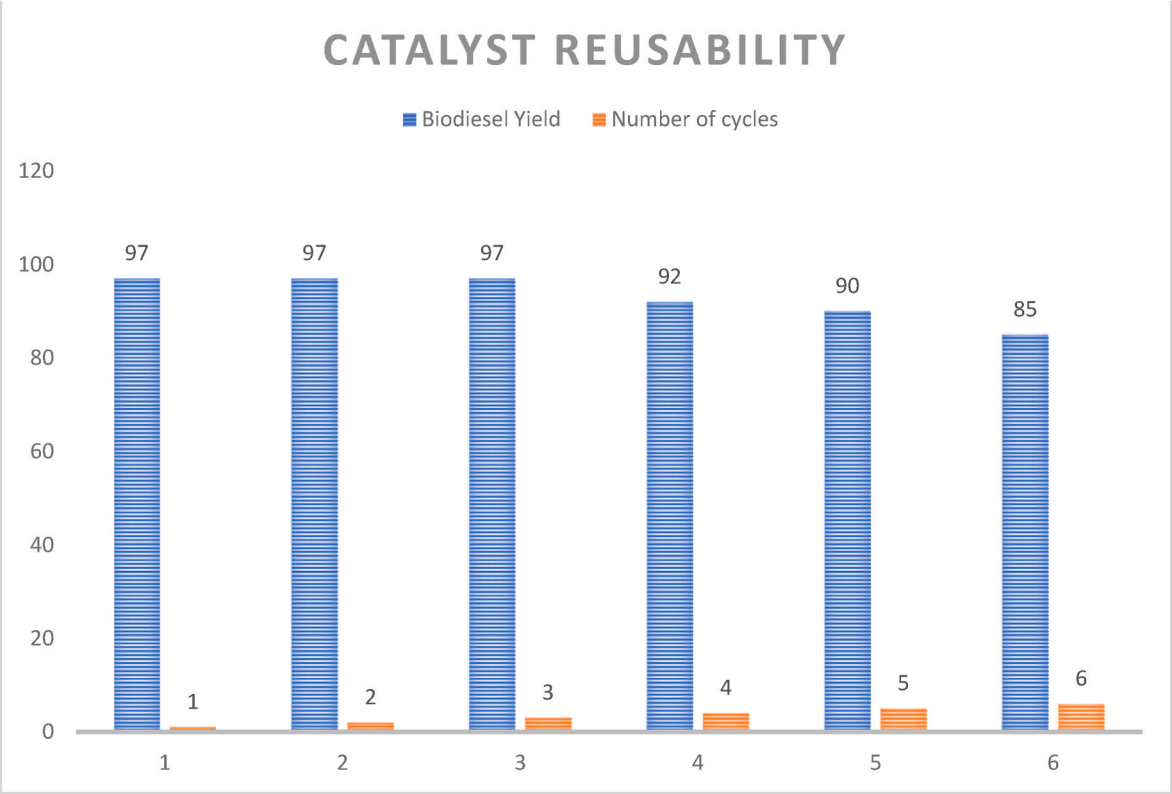

Fig. 7. Reusability of Sodium/Potassium Oxide Nano catalyst.

cycle yield decreased up to 92%, 90% and 85% successively due to sedimentation of organic matter present in reaction mixture of transesterification. However, through repeated washing and calcination catalytic efficiency of the nano catalysts can be recovered. Reusability is the key towards the prosperity of economy and environment. The graphic presentation of bimetallic catalyst is given in Fig. 7.

4. Conclusion, future, limitation and challenging

Focusing on the current defaults of environmental toxicity, the uprising globe's temperature, and waste management, and circular economy, the exploration of novel non-edible, toxic, and waste feedstock for renewable biodiesel synthesis is the need of the hour. Environmental toxicology, elevated temperature, climate change and sea level rising in the current era is directly linked with greenhouse gases release by fossil fuels burning. Environmental and economic situation can be improved by accepting the organic and greener side of energy production and utilization of waste material. The conventional linear system of economy is no more effective in reducing energy, environmental and economic crises as there is no way of recycling and circulation. Fossil fuels are depleting at exponential rate as the population of world is going to increases day by day. Hazardous and non-edible seeds of plants are wasted every season by falling on the ground. In the current situation of energy crises and high fuel prices, it is the need of the hour to utilize these non-edible hazardous seeds for biodiesel production. Investment of waste and hazardous biological resources will bring prosperity in economic conditions, waste management and environmental situation worldwide. This circular economic strategy will combat the linear way of energy production and will bring positive change in the form of re-utilization, recycling, and the investment of waste and hazardous materials. Biodiesel production from waste, non-edible and hazardous sources are scientifically proven as environment-friendly, free of pollutants, hazardous and greenhouse gases. Sustainable developmental goals can be achieved through clean, renewable, and green energy production. Circular way of energy production and reusability is the solution the environmental problems and fossil fuels diminution. The seeds of *Buxus papillosa* are wasted in every season due to their toxicity. Utilization of waste, hazardous and toxic seeds of *Buxus papillosa* for sustainable biodiesel production could be commercialized in future for a sustainable energy. The efficiency of *Buxus papillosa* seed oil content, its conversion to biodiesel along with the novel sodium potassium green nanocatalyst is compared with the past research from literature in Table 7. Greenhouse gases and fossil fuels utilization could be minimized by this alternative circular economic strategy in the form of green fuel (biodiesel). Development of biofuel industries in accordance with circular economic strategies will lead to reduction in fossil fuels utilization and environmental toxicity, creation of social and economic opportunities, more research and development in the field of bio-energy

Table 7
A comparative study of plant seed oil content, green nanocatalyst and biodiesel yield.

Source	Oil content	Plant Based Membrane Catalyst	Obtained yield (%)	References
Buxus papillosa	45%	sodium/ potassium oxide	97%	Present case
Cannabis sativa	34%	Bismuth oxide	92%	(Sawaira et al., 2023)
Monotheca buxifolia	45%	Calcium oxide	95%	Rozina et al. (2022)
Diospyros malabarica	39%	Cadmium oxide	94%	Arshad et al. (2023)
Citrus aurantium	38%	zirconium oxide	94%	(Rozina, Ahmad, & Zafar, 2021)
Acacia furnesiana	22.8%	Nickel ferrite oxide	93.1%	(Kattimani, Yatish, Pramoda, Sakar and Balakrishna, 2023)

and waste investment. Worldwide efforts and strategies are required to be made for waste material utilization for biofuel and biodiesel production as a clean and green technology combating the environmental and economic issues. Adaptation, installation, and improvement of renewable and circular economical technologies must be done worldwide for a prosperous, pollution free and sustainable world. The main concern of the currently conducted research is to acquaint more novel feedstocks for ecologically sustaining and remedial biodiesel for environment healing and recycling-ability and waste investment for economic prosperity.

- Investment of *Buxus papillosa* seeds that are usually wasted every season for the economical upgradation, sustainability, and environment healing.
- Utilization of novel salt sodium potassium tartrate along with novel aqueous extract of *Buxus papillosa* fruit capsule to avoid any wastage for novel Phyto-nanocatalyst sodium/potassium oxide.
- The unadulterated and nano-nature of sodium/potassium oxide was authenticated through different innovative tools of characterization.
- Optimal reaction conditions of 8:1 (alcohol: oil), newly synthesized bimetallic nanocatalyst amount (0.37 wt%), temperature (80 °C) for 180 duration of time ended in highest yield output of 97%.
- The catalytic activity of the novel Phyto-nanocatalyst sodium/potassium oxide was up to six levels.
- *Buxus papillosa* seed oil's successful conversion to bio-diesel was ascertained by FT-IR, GC/MS, and NMR modern analytical approaches. GC/MS unveiled 17 methylated ester compounds in the BPBD sample.
- *Buxus papillosa* bio-diesel has fuel physical properties matched with international fuel limits. For example, BPBD has sulphur concentrations (0.0009%), acidic value (0.32 mg KOH/g), pour point (−9 °C), kinematic density (0.89 kg/m^3), viscosity (5.01 mm^2/s), flash, and cloud points 75 °C and −8 °C respectively.
- The evaluated study signifies that *Buxus papillosa* having high seeds oil concentration (45%) is the inedible, waste, toxic, and novel feedstock for non-hazardous biodiesel synthesis. Utilization of waste and toxic sources for non-toxic bio-diesel formation is the need of the hour in the current depleting environment and economic crises to improve the natural ability of Earth planet, economical sustainability and converting the trend to organic way of life.

Credit author statement

Ikram Faiz, Mushtaq Ahmad: Conception and design of study; Supervision of work; Acquisition, analysis and interpretation of data, Mohamed Fawzy Ramadan, Muhammad Zafar, Ulfat Zia: Drafting of the manuscript, Rozina, Awais Bokhari, Sasan Zahmatkesh: Curation/Resources, Writing original Draft/Review& Editing, Methodology/Supervision, Resources/Editing. Saira Asif, Bing-Jie Ni: Writing original Draft/Review& Editing.

Statements and declarations

Our present research is pure scientific work and we do not have any financial interests and benefits related to this research.

Funding

The Deputyship for Research & Innovation, Ministry of Education in Saudi Arabia, Project number: IFP22UQU4430043DSR117.

Declaration of competing interest

The authors declare that they have no known competing financial interests or personal relationships that could have appeared to influence the work reported in this paper.

Data availability

No data was used for the research described in the article.

Acknowledgment

The authors extend their appreciation to the Deputyship for Research & Innovation, Ministry of Education in Saudi Arabia for funding this research work through the project number: IFP22UQU4430043DSR117.

References

Ahmad, F., 2022. Deep image retrieval using artificial neural network interpolation and indexing based on similarity measurement. CAAI Trans. Intelligence Tech. 7 (2), 200–218.
Aikhuele, D., 2023. Development of a statistical reliability-based model for the estimation and optimization of a spur gear system. J. Comput. Cognitive Eng. 2 (2), 168–174.
Abbasi, T.U., Ahmad, M., Asma, M., Munir, M., Zafar, M., Katubi, K.M., Alsaiari, N.S., Yahya, A.E., Mubashir, M., Chuah, L.F., 2023. High efficient conversion of Cannabis sativa L. biomass into bioenergy by using green tungsten oxide nano-catalyst towards carbon neutrality. Fuel 336, 126796.
Abdelmigeed, M.O., Al-Sakkari, E.G., Hefney, M.S., Ismail, F.M., Ahmed, T.S., Ismail, I. M., 2021. Biodiesel production catalyzed by NaOH/Magnetized ZIF-8: yield improvement using methanolysis and catalyst reusability enhancement. Renew. Energy 174, 253–261.
Abdullah, R.F., Rashid, U., Ibrahim, M.L., Hazmi, B., Alharthi, F.A., Nehdi, I.A., 2021. Bifunctional nano-catalyst produced from palm kernel shell via hydrothermal-assisted carbonization for biodiesel production from waste cooking oil. Renew. Sustain. Energy Rev. 137, 110638.
Ahmad, M., Alruqi, M., Zafar, M., 2022a. Cleaner production of biodiesel from novel and non-edible seed oil of Chamaerops humilis using recyclable cobalt oxide nanoparticles: a contribution to resilient and sustainable world. J. Clean. Prod. 369, 133378.
Ahmad, M., Elnaggar, A.Y., Teong, L.K., Sultana, S., Zafar, M., Munir, M., Hussein, E.E., Abidin, S.Z.U., 2022b. Sustainable and eco-friendly synthesis of biodiesel from novel and non-edible seed oil of Monotheca buxifolia using green nano-catalyst of calcium oxide. Energy Convers. Manag. X 13, 100142.
Alsaiari, M., Ahmad, M., Munir, M., Zafar, M., Sultana, S., Dawood, S., Almohana, A.I., MH, A.-M.H., Alharbi, A.F., Ahmad, Z., 2023a. Efficient application of newly synthesized green Bi2O3 nanoparticles for sustainable biodiesel production via membrane reactor. Chemosphere 310, 136838.
Alsaiari, M., Ahmad, M., Zafar, M., Harraz, F.A., Algethami, J.S., Šljukić, B., Santos, D. M., Akhtar, M.S., 2023b. Transformation of waste seed biomass of Cordia myxa into valuable bioenergy through membrane bioreactor using green nanoparticles of indium oxide. Chemosphere 314, 137604.
Alsaiari, M., Ahmad, M., Zafar, M., Sultana, S., Rizk, M.A., Almohana, A.I., Ahmad, Z., Alsaiari, R.A., Akhtar, M.S., 2022. Treatment of Saussurea heteromalla for biofuel synthesis using catalytic membrane reactor. Chemosphere 305, 135335.
Ameen, M., Zafar, M., Ramadan, M.F., Ahmad, M., Makhkamov, T., Bokhari, A., Mubashir, M., Chuah, L.F., Show, P.L., 2023. Conversion of novel non-edible Bischofia javanica seed oil into methyl ester via recyclable zirconia-based phyto-nanocatalyst: a circular bioeconomy approach for eco-sustenance. Environ. Technol. Innovat. 30, 103101.
Arora, N.K., Mishra, I., 2022. Current scenario and future directions for sustainable development goal 2: a roadmap to zero hunger. Environ. Sustain. 5, 129–133.
Arshad, S., Ahmad, M., Munir, M., Sultana, S., Zafar, M., Dawood, S., Alghamdi, A.M., Asif, S., Bokhari, A., Mubashir, M., 2023. Assessing the potential of green CdO2 nano-catalyst for the synthesis of biodiesel using non-edible seed oil of Malabar Ebony. Fuel 333, 126492.
Bhatia, S.K., Bhatia, R.K., Jeon, J.-M., Pugazhendhi, A., Awasthi, M.K., Kumar, D., Kumar, G., Yoon, J.-J., Yang, Y.-H., 2021. An overview on advancements in biobased transesterification methods for biodiesel production: oil resources, extraction, biocatalysts, and process intensification technologies. Fuel 285, 119117.
Borah, M.J., Devi, A., Borah, R., Deka, D., 2019. Synthesis and application of Co doped ZnO as heterogeneous nanocatalyst for biodiesel production from non-edible oil. Renew. Energy 133, 512–519.
Buhr, E., Senftleben, N., Klein, T., Bergmann, D., Gnieser, D., Frase, C.G., Bosse, H., 2009. Characterization of nanoparticles by scanning electron microscopy in transmission mode. Meas. Sci. Technol. 20, 084025.
Chaudhry, B., Akhtar, M.S., Ahmad, M., Munir, M., Zafar, M., Alhajeri, N.S., Al-Muhtaseb, A.a.H., Ahmad, Z., Hasan, M., Bokhari, A., 2022. Membrane based reactors for sustainable treatment of Coronopus didymus L. by developing Iodine doped potassium oxide Catalyst under Dynamic conditions. Chemosphere 303, 135138.
Clogston, J.D., Patri, A.K., 2011. Zeta Potential Measurement. Characterization of Nanoparticles Intended for Drug Delivery, pp. 63–70.
Dawood, S., Ahmad, M., Zafar, M., Asif, S., Klemeš, J.J., Bokhari, A., Mubashir, M., Han, N., Ibrahim, M.M., El-Bahy, Z.M., 2022. Biodiesel synthesis from Prunus bokhariensis non-edible seed oil by using green silver oxide nanocatalyst. Chemosphere 291, 132780.

Dawood, S., Koyande, A.K., Ahmad, M., Mubashir, M., Asif, S., Klemeš, J.J., Bokhari, A., Saqib, S., Lee, M., Qyyum, M.A., 2021. Synthesis of biodiesel from non-edible (Brachychiton populneus) oil in the presence of nickel oxide nanocatalyst: parametric and optimisation studies. Chemosphere 278, 130469.
Devi, S., 2022. Pakistan floods: impact on food security and health systems. Lancet 400, 799–800.
Di Serio, M., Tesser, R., Pengmei, L., Santacesaria, E., 2008. Heterogeneous catalysts for biodiesel production. Energy Fuels 22, 207–217.
Diehl, B., Randel, G., 2007. Analysis of biodiesel, diesel and gasoline by NMR spectroscopy–a quick and robust alternative to NIR and GC. Lipid Technol. 19, 258–260.
Dubé, M., Tremblay, A., Liu, J., 2007. Biodiesel production using a membrane reactor. Bioresour. Technol. 98, 639–647.
Durner, G.M., Douglas, D.C., Nielson, R.M., Amstrup, S.C., McDonald, T.L., Stirling, I., Mauritzen, M., Born, E.W., Wiig, Ø., DeWeaver, E., 2009. Predicting 21st-century polar bear habitat distribution from global climate models. Ecol. Monogr. 79, 25–58.
Deng, C., Zhang, L., Deng, H., 2022. Improving sentence simplification model with ordered neurons network. CAAI Trans. Intelligence Tech. 7 (2), 268–277.
Endalew, A.K., Kiros, Y., Zanzi, R., 2011. Inorganic heterogeneous catalysts for biodiesel production from vegetable oils. Biomass Bioenergy 35, 3787–3809.
Ewing, M., Msangi, S., 2009. Biofuels production in developing countries: assessing tradeoffs in welfare and food security. Environ. Sci. Pol. 12, 520–528.
Fadhil, A.B., Saleh, L.A., Altamer, D.H., 2020. Production of biodiesel from non-edible oil, wild mustard (Brassica Juncea L.) seed oil through cleaner routes. Energy Sources, Part A Recovery, Util. Environ. Eff. 42, 1831–1843.
Gómez-Trejo-López, E., González-Díaz, M.O., Aguilar-Vega, M., 2022. Waste cooking oil transesterification by sulfonated polyphenylsulfone catalytic membrane: characterization and biodiesel production yield. Renew. Energy 182, 1219–1227.
Gupta, H., 2010. Qualitative and quantitative microscopial studies on Buxus papillosa Schneider. J. Econ. Taxon. Bot. 34, 517–520.
He, C., Zhou, T., Zhang, L., Chen, X., Zhang, W., 2023. Extremely hot East Asia and flooding western South Asia in the summer of 2022 tied to reversed flow over Tibetan Plateau. Clim. Dynam. 1–17.
Hu, X., Kuang, Q., Cai, Q., Xue, Y., Zhou, W., Li, Y., 2022. A coherent pattern mining algorithm based on all contiguous column bicluster. J. Artificial Intelligence and Tech. 2 (3), 80–92.
Ibrahim, N.A., Rashid, U., Hazmi, B., Moser, B.R., Alharthi, F.A., Rokhum, S.L., Ngamcharussrivichai, C., 2022. Biodiesel production from waste cooking oil using magnetic bifunctional calcium and iron oxide nanocatalysts derived from empty fruit bunch. Fuel 317, 123525.
Ingham, B., 2015. X-ray scattering characterisation of nanoparticles. Crystallogr. Rev. 21, 229–303.
Jayakumar, M., Karmegam, N., Gundupalli, M.P., Gebeyehu, K.B., Asfaw, B.T., Chang, S. W., Ravindran, B., Awasthi, M.K., 2021. Heterogeneous base catalysts: synthesis and application for biodiesel production–A review. Bioresour. Technol. 331, 125054.
Kambo, H.S., Dutta, A., 2015. A comparative review of biochar and hydrochar in terms of production, physico-chemical properties and applications. Renew. Sustain. Energy Rev. 45, 359–378.
Knothe, G., Steidley, K.R., 2005. Kinematic viscosity of biodiesel fuel components and related compounds. Influence of compound structure and comparison to petrodiesel fuel components. Fuel 84, 1059–1065.
Koria, L., Nithya, G., 2012. Analysis of Datura stramonium Linn. biodiesel by gas chromatography-mass spectrometry (gc-ms) and influence of fatty acid composition on the fuel related characteristics. J. Phytol. 4, 6–9.
Kumar, R., Ghosh, A.K., Pal, P., 2020. Synergy of biofuel production with waste remediation along with value-added co-products recovery through microalgae cultivation: a review of membrane-integrated green approach. Sci. Total Environ. 698, 134169.
Kurowska, K., Marks-Bielska, R., Bielski, S., Kryszk, H., Jasinskas, A., 2020. Food security in the context of liquid biofuels production. Energies 13, 6247.
Landi Jr., S., Segundo, I.R., Freitas, E., Vasilevskiy, M., Carneiro, J., Tavares, C.J., 2022. Use and misuse of the Kubelka-Munk function to obtain the band gap energy from diffuse reflectance measurements. Solid State Commun. 341, 114573.
Lin, C.-Y., Lin, H.-A., Hung, L.-B., 2006. Fuel structure and properties of biodiesel produced by the peroxidation process. Fuel 85, 1743–1749.
Mahlknecht, J., González-Bravo, R., Loge, F.J., 2020. Water-energy-food security: a Nexus perspective of the current situation in Latin America and the Caribbean. Energy 194, 116824.
Marchetti, J., Miguel, V., Errazu, A., 2007. Possible methods for biodiesel production. Renew. Sustain. Energy Rev. 11, 1300–1311.
Moyo, L., Iyuke, S., Muvhiiwa, R., Simate, G., Hlabangana, N., 2021. Application of response surface methodology for optimization of biodiesel production parameters from waste cooking oil using a membrane reactor. South Afr. J. Chem. Eng. 35, 1–7.
Munir, M., Saeed, M., Ahmad, M., Waseem, A., Alsaady, M., Asif, S., Ahmed, A., Shariq Khan, M., Bokhari, A., Mubashir, M., Fatt Chuah, L., Loke Show, P., 2023. Cleaner production of biodiesel from novel non-edible seed oil (Carthamus lanatus L.) via highly reactive and recyclable green nano CoWO3@rGO composite in context of green energy adaptation. Fuel 332, 126265.
Meng, J., Li, Y., Liang, H., Ma, Y., 2022. Single-image dehazing based on two-stream convolutional neural network. J. Artificial Intelligence and Tech. 2 (3), 100–110.
Nabipour, N., Daneshfar, R., Rezvanjou, O., Mohammadi-Khanaposhtani, M., Baghban, A., Xiong, Q., Li, L.K., Habibzadeh, S., Doranehgard, M.H., 2020. Estimating biofuel density via a soft computing approach based on intermolecular interactions. Renew. Energy 152, 1086–1098.
Nayan, V., Onteru, S.K., Singh, D., 2018. Mangifera indica flower extract mediated biogenic green gold nanoparticles: efficient nanocatalyst for reduction of 4-nitrophenol. Environ. Prog. Sustain. Energy 37, 283–294.
Ramírez Verduzco, L.F., 2013. Density and viscosity of biodiesel as a function of temperature: empirical models. Renew. Sustain. Energy Rev. 19, 652–665.
Rozina, Ahmad, M., Elnaggar, A.Y., Keat Teong, L., Sultana, S., Zafar, M., Munir, M., Hussein, E.E., Zain Ul Abidin, S., 2022. Sustainable and eco-friendly synthesis of biodiesel from novel and non-edible seed oil of Monotheca buxifolia using green nano-catalyst of calcium oxide. Energy Convers. Manag. X 13, 100142.
Saleem, H., Khurshid, U., Anwar, S., Tousif, M.I., Mahomoodally, F.M., Ahemad, N., 2022. Buxus papillosa CK Schneid.: a comprehensive review on traditional uses, botany, phytochemistry, pharmacology, and toxicology. Biocatal. Agric. Biotechnol., 102547
Samuel, O.D., Oreko, B.U., Oyejide, J.O., Idi, S., Fayomi, O.S.I., 2019. Experimental and empirical study of diesel and biodiesel produced from blend of fresh vegetable and waste vegetable oil on density, viscosity, sulphur content and acid value. J. Phys. Conf. 1378, 042024.
Sanjay, B., 2013. Heterogeneous catalyst derived from natural resources for biodiesel production: a review. Res. J. Chem. Sci. ISSN 2231, 606X.
Santos, S.M., Nascimento, D.C., Costa, M.C., Neto, A.M.B., Fregolente, L.V., 2020. Flash point prediction: reviewing empirical models for hydrocarbons, petroleum fraction, biodiesel, and blends. Fuel 263, 116375.
Siddiqi, M.H., Liu, X.-m., Qureshi, T., Tabish, A.N., Nawaz, S., Iqbal, T., 2020. Performance analysis of bio-fuel blends for clean energy production: thermogravimetric analysis. J. Clean. Prod. 273, 122936.
Soontarapa, K., Ampairojanawong, R., Palakul, T., 2023. Esterification and transesterification of palm fatty acid distillate in chitosan membrane reactor. Fuel 339, 126918.
Torrent, J., Barrón, V., 2008. Diffuse reflectance spectroscopy. Methods of Soil Analysis Part 5—Mineralogical Methods 5, 367–385.
Udmale, P., Pal, I., Szabo, S., Pramanik, M., Large, A., 2020. Global food security in the context of COVID-19: a scenario-based exploratory analysis. Progress in Disaster Science 7, 100120.
Wang, H., Tang, H., Wilson, J., Salley, S.O., Ng, K.S., 2008. Total acid number determination of biodiesel and biodiesel blends. J. Am. Oil Chem. Soc. 85, 1083–1086.
Wang, J., Yang, L., Luo, W., Yang, G., Miao, C., Fu, J., Xing, S., Fan, P., Lv, P., Wang, Z., 2017. Sustainable biodiesel production via transesterification by using recyclable Ca2MgSi2O7 catalyst. Fuel 196, 306–313.
Wang, R., Zhou, W.-W., Hanna, M.A., Zhang, Y.-P., Bhadury, P.S., Wang, Y., Song, B.-A., Yang, S., 2012. Biodiesel preparation, optimization, and fuel properties from non-edible feedstock. Datura stramonium L. Fuel 91, 182–186.
Wang, Y.Q., Li, J.Y., Chen, C.H., Zhang, J., Zhan, Z.H., 2023. Scale adaptive fitness evaluation-based particle swarm optimisation for hyperparameter and architecture optimisation in neural networks and deep learning. CAAI Trans. Intelligence Tech. 8 (3), 849–862.
Yaşar, F., 2020. Comparision of fuel properties of biodiesel fuels produced from different oils to determine the most suitable feedstock type. Fuel 264, 116817.
Yesilyurt, M.K., Cesur, C., 2020. Biodiesel synthesis from Styrax officinalis L. seed oil as a novel and potential non-edible feedstock: a parametric optimization study through the Taguchi technique. Fuel 265, 117025.
Zhang, Y., Niu, S., Lu, C., Gong, Z., Hu, X., 2020. Catalytic performance of NaAlO2/γ-Al2O3 as heterogeneous nanocatalyst for biodiesel production: optimization using response surface methodology. Energy Convers. Manag. 203, 112263.